

Structure Formation in the Universe with Quantum Gravity Cutoff

Sven Ahrens
2008



TECHNISCHE
UNIVERSITÄT
DARMSTADT

Technical University Darmstadt
in cooperation with:
Ruprecht Karls University Heidelberg
Center for Astronomy (ZAH)
Landessternwarte (LSW)
Theory Group

Abstract

In this Masterthesis the structure formation process in the early universe is considered. At the end the measured power spectra of the cosmological structure are compared with the predicted power spectra, having a focus on a observable deviation.

The investigations are based on the Λ CDM-Model (also called Concordance-Model of Cosmology), using the latest cosmological parameters obtained from WMAP and others [21]. The evolution of the primordial density perturbations, described by cosmological perturbation theory, are calculated with `cmbeasy`. `cmbeasy` is also used for investigating the influence of a cutoff in the primordial power spectrum in the CMB. The non-linear correction of the power spectrum is worked out and applied on perturbations which enter the non-linear regime. The power spectrum of the structures in the universe are compared with the expected power spectra from theory. On the large scales there seems to be no cutoff in the observed power spectrum. In the luminosity function of galaxies one might conclude a cutoff at a scale of about $\lambda = 100kpc$. Especially the nonexistence of a huge number of dark matter halo objects, which should exist according to [43] raises the suspicion, that primordial fluctuations were never been produced on small scales during inflation.



Contents

1	Introduction	5
2	Equivalence Principles and General Relativity	7
2.1	Weak Equivalence Principle	7
2.2	Einstein's Equivalence Principle	7
2.3	Strong Equivalence Principle	8
3	Differential Geometry of Spacetime	9
3.1	Notion of a manifold	9
3.2	The Tangent Space and One-Forms	9
3.3	Tensors and their transformation behavior	10
3.4	Differential Forms	11
3.5	The Connection	12
3.5.1	Geometric interpretation	12
3.5.2	Definition and properties	12
3.5.3	Component representation	13
3.5.4	The generalized divergence	13
3.6	The Metric	13
3.7	Torsion and Curvature	14
3.8	Resulting relations	14
3.8.1	Identities	14
3.8.2	The Levi-Civita connection	15
3.9	The Cartan Structure Equations	15
3.10	Conformal Transformations	15
4	The Homogeneous Universe	17
4.1	Einstein's Field Equations	17
4.2	Using symmetries	17
4.3	Friedmann-Robertson-Walker space-time	19
4.4	Scale factor and Redshift	20
4.5	Distance and angular width	21
4.6	The Friedmann Equations	22
4.6.1	Density evolution	22
4.7	Density Parameters	23
4.7.1	Values of the density parameters	24
4.8	Inflation	26
4.8.1	A typical inflationary universe	27
4.9	The Horizon Scale	27
5	Cosmological Perturbation Theory	29
5.1	Perturbations of the background quantities	29
5.1.1	Metric perturbations	29
5.1.2	Perturbations of the energy momentum tensor	30
5.2	Initial Conditions	32
6	The cmbeasy program	33
6.1	Short description	33
6.2	Configuration and Properties	33
6.3	The Evolution of Perturbations	33
7	Power Spectra	41



7.1	Conventions	41
7.2	Comparison with measurements	42
7.3	Evolution of the power spectrum	43
7.3.1	The Transferfunction	43
7.3.2	Nonlinear growth	44
8	The search for a cutoff	47
8.1	The CMB	47
8.2	CDM power spectra	47
8.3	Luminosity function of galaxies	50
8.4	Discussion	50
8.4.1	Conventional generation of fluctuations	52
8.4.2	Conclusions	53
9	Acknowledgements	55

1 Introduction

At high energies the centrifugal force of particles in a ring accelerator grows linear with their kinetic energy. If conventional accelerator technology is used, the size of a particle accelerator will therefore grow linear with the desired particle energy. As a result it may be more difficult to justify accelerator experiments of higher and higher energies to the commonality in some future, specially against the background of the future development of energy availability. On this account non-accelerator experiments are getting more important for verifying theories beyond the standard model of particle physics and general relativity.

The physics of the big bang opens another observational window to Planck-scale physics. Though Planck-scale physics happens at energies, scales and temperatures, where quantum physics and general relativity are both in conflict with each other a quantum gravity cutoff should be apparent. In the standard cosmological model the universe has expanded from a very small extension to the size of 13.7 billion light-years today. Especially inflation, the 'first' stage of the universe, during which a growth of about 30 orders of magnitude happened, provides a window towards trans-Planckian physics as it magnifies all quantum fluctuations down to scales which can easily be observed today.

The great unification of quantum field theory and general relativity has not been done till today in a convincing way. Approaches to this unification are done by string theory and other theories of quantum gravity. There are anyhow a lot of unfixed parameters and unresolved problems with these theories.

Especially the question arises:

What is the smallest structure in physics?

This work tries to give an answer to this question by considering the observational data of the universe. By investigating the cosmic microwave background radiation (CMBR) and the spatial mass and structure distribution of the universe the mentioned trans-Planckian physics may be resolved. Especially some kind of quantum gravity cutoff can be concluded from the existence of structure in the universe.

The plan of this work is the following:

First there are some notes on the equivalence principles in general relativity. In chapter 3 the formalism of differential geometry is worked out. The explanations of differential geometry are concentrating on their application on Friedmann-Robertson-Walker space-times, which are treated in chapter 4. In this chapter the Friedmann cosmology and an easy inflation model are considered. The expansion laws of different matter species are noted and correlated to Hubble's law. A comparison of two notations of horizons is done with the result, that $Ha \approx \tau^{-1}$ approximately holds. After that, chapter 5 continues with a summary on cosmological perturbation theory, where the Einstein equations are linearized and perturbed over a homogeneous FRW-background. The (adiabatic) initial conditions of the perturbation variables are discussed. The initial conditions are important to introduce a cutoff in the power spectrum, by using `cmbeasy`, which will be documented in chapter 6. This chapter is focussed on the evolution of the density perturbation variables at small scales (high k). The next chapter 7 tries to give consistency relations between the different power spectra and the last chapter uses the power spectra to find an observational cutoff in the temperature anisotropy power spectrum of the CMB, the galaxy power spectrum of the SDSS and intergalactic medium, and the luminosity function of galaxies. At the end the results are discussed.



2 Equivalence Principles and General Relativity

Since its publication by Einstein in 1915 the Theory of General Relativity (GR) seems to be the theory which describes gravity in the correct manner. However small deviations of GR may give an evidence for generalized unified theories. These irregularities can be measured as deviations of the equivalence principles, which are explained in the following. For a detailed discussion about equivalence principles see [1], which is the source of this section.

2.1 Weak Equivalence Principle

The Weak Equivalence Principle (WEP) states that the passive mass m_p , which is affected by the gravitational force is proportional to the inertial mass m_i , which appears as force during acceleration.

If WEP holds then two different bodies have the same acceleration in an external gravitational field (also called Universality of Free Fall (UFF)). An alternative statement of WEP is that the trajectory of a freely falling test body is independent of its internal structure and composition. The WEP is measured by the difference of the accelerations of two different test bodies divided by their sum of accelerations [1]:

$$\eta = 2 \frac{|a_1 - a_2|}{|a_1 + a_2|} \quad (2.1)$$

The best limit measured until now is $\eta < 3 \cdot 10^{-13}$. Future experiments would reach lower bounds of $\eta < 10^{-13}$ on the Earth surface and $\eta < 10^{-17}$ in space.

2.2 Einstein's Equivalence Principle

Before discussing Einsteins Equivalence Principle (EEP) two concepts have to be introduced:

- The Local Lorentz Invariance (LLI) states that every non-gravitational, physical process has to be locally independent of the inertial system. So the process has to be invariant under Lorentz transformations. LLI is measured as deviation of the speed of light [1]:

$$\delta = |c^{-2} - 1| \quad (2.2)$$

Current measurements give bounds of $\delta < 10^{-20}$.

- The Local Position Invariance (LPI) states that every non-gravitational, physical process has to be independent of its spacelike and timelike position. Especially physical constants have to be the same everywhere. The accuracy of LPI is measured as the redshift of two bodies in a comoving frame in a gravitational potential:

$$\frac{\delta\nu}{\nu} = Z = (1 + \alpha) \frac{\Delta U}{c^2}, \quad (2.3)$$

where the equation is correct if $\alpha = 0$. Experimental lower bounds on α are $< 10^{-4}$. It is also possible to investigate the rate of change of some natural constants like the electromagnetic fine structure constant, the electron-proton mass ratio, or the gyromagnetic ratio of the proton. The ratio of the change of the constant divided by the constant itself is measured in the range of 10^{-16} for some experiments.

Einsteins Equivalence Principle states that WEP, LLI and LPI are valid.

If these assumptions are fulfilled and there is no force acting on test bodies, they are moving locally in straight lines, which will be geodesics globally in the curved spacetime. So if EEP is valid, then the underlying theory must be a "metric theory of gravity", which satisfies the postulates:

-
1. Spacetime is endowed with a symmetric metric.
 2. The trajectories of freely falling test bodies are geodesics of that metric.
 3. In locally freely falling reference frames, the non-gravitational laws of physics are those written in the language of special relativity.

2.3 Strong Equivalence Principle

The Strong Equivalence Principle (SEP) states that EEP is valid and additionally WEP is also valid for self-gravitating bodies.

There is no rigorous proof, but one can argue, that if SEP is valid then the only gravitational field, which can exist, is the metric g . Empirically it has been found that almost every metric theory other than GR introduces auxiliary gravitational fields and thus predicts violations of SEP at some level. General relativity seems to be the only viable metric theory that embodies SEP completely.

3 Differential Geometry of Spacetime

3.1 Notion of a manifold

There exists a lot of literature on differential geometry [5], [6], [7], [12], [13]. In this chapter a summary of the important contents is given, which has not the demand to be fully complete in mathematical sense. A well-founded description of differential geometry can be found in [2], which is primarily taken into account.

For obtaining the 4 dimensional Riemannian space of general relativity some structures are introduced. The first structure is the manifold:

Definition 3.1.1 (Manifold). A manifold of dimension 4 is a topological space such that around each point there exists a neighborhood which is homeomorphic to an open subset of \mathbb{R}^4 .

This means that for a point p in a manifold M there always exist local coordinates (x^1, x^2, x^3, x^4) in the neighborhood of $p \in M$ ¹ and a continuous and bijective (homeomorphic) mapping $h : M^4 \rightarrow \mathbb{R}^4$. The mappings h are called **charts**. If the whole manifold is patched together with these charts their set is called an **atlas**. If the mappings h are differentiable and bijective these **diffeomorphisms** are called **diffeomorph**. In the future it is always assumed that the mappings are C^∞ - diffeomorph (C^∞ is also called **smooth**).

3.2 The Tangent Space and One-Forms

Now consider a smooth curve $c : \mathbb{R} \rightarrow M^4$ with $c(0) = p$.

Definition 3.2.1 (Tangential Vector). A tangential vector is defined as:

$$v = \left. \frac{d}{dt}(h \circ c) \right|_{t=0} = \left. \frac{d}{dt}[h(c(t))] \right|_{t=0} \quad (3.1)$$

Written in components one obtains:

$$v^i = \left. \frac{\partial h^i(c(t))}{\partial c^j(t)} \frac{dc^j(t)}{dt} \right|_{t=0} = \left. \frac{dc^j(t)}{dt} \right|_{t=0} \left. \frac{\partial}{\partial x^j} h^i(x) \right|_{x=p} \quad (3.2)$$

One can verify that the tangential vectors build a vector space in \mathbb{R}^4 . A basis of this **tangential space** $T_p(M)$ is the derivative of the local coordinates: $\frac{\partial}{\partial x^j} = \partial_j$. The curve can then be decomposed into coefficients of their tangential vector:

$$X^j = \left. \frac{dc^j(t)}{dt} \right|_{t=0} \quad (3.3)$$

$X = X^j \partial_j$ is a **derivation** whose action on smooth functions $f, g : M \rightarrow \mathbb{R}$ is noted as

$$X(f) := X.f := X^j \partial_j f \quad (3.4)$$

and fulfills the Leibniz Rule:

$$X.(fg) = gX.f + fX.g \quad (3.5)$$

The set of all tangential vectors is the tangential space: $X \in T_p(M)$.

Definition 3.2.2 (Differential). Let $f : M \rightarrow \mathbb{R}$ be a smooth function and $X \in T_p(M)$. The differential df is a mapping $(df)_p : T_p(M) \rightarrow \mathbb{R}$ defined by:

$$(df)_p(X) := X(f) = X.f \quad (3.6)$$

¹ The upper index n of the manifold declares the number of local coordinates.

One can see, that the differentials build a vector space too, which is named **cotangent space** or **dual space**. In particular, the component functions $x^i : M^4 \rightarrow \mathbb{R}$, $x_i(x_1, x_2, x_3, x_4) = x_i$ satisfy

$$(dx_i)(\partial_j) = \partial_j x^i = \langle dx^i, \partial_j \rangle = \delta_j^i, \quad (3.7)$$

which is the reason, why the dx^i are said to be the basis of the **dual base** $T_p^*(M)$. The corresponding ‘vector’ in the dual space $\omega = \omega_i dx^i \in T_p^*(M)$ is called a one-form.

Definition 3.2.3 (Vector Field). Let $p \in M$ be a point of a manifold M . The mapping $X : p \rightarrow X_p$ is called a **vector field** on M . The set of all smooth (C^∞) vector fields on M is denoted by $\mathcal{X}(M)$. The set of all smooth mappings $\omega : p \rightarrow \omega_p$ of one-forms on M is denoted by $\mathcal{X}^*(M)$

In local coordinates (x_1, x_2, x_3, x_4) of an open subset $U \in M$, $\mathcal{X}(M)$ and $\mathcal{X}^*(M)$ have the representations:

$$X_p = \xi^i(p) \left(\frac{\partial}{\partial x^i} \right)_p \in \mathcal{X}(M) \quad \omega_p = \zeta_i(p) (dx^i)_p \in \mathcal{X}^*(M) \quad (3.8)$$

3.3 Tensors and their transformation behavior

Let $X = X^i \frac{\partial}{\partial x^i} \in \mathcal{X}(M)$ be a vector and $\omega = \omega_i dx^i \in \mathcal{X}^*(M)$ a one-form. Under the change of coordinates given by the mapping $x' : M^4 \rightarrow N^4$, $x'^i(x^1, x^2, x^3, x^4)$, $x'(p) = q$ the vectors transform in the following way:

$$X \cdot x^{i'} = X^j \frac{\partial}{\partial x^j} x^{i'} = X^j \frac{\partial x^{k'}}{\partial x^j} \delta_{k'}^{i'} = \frac{\partial x^{k'}}{\partial x^j} X^j \frac{\partial x^{i'}}{\partial x^{k'}} = X^{k'} \frac{\partial}{\partial x^{k'}} x^{i'} \quad (3.9)$$

$$\omega \left(\frac{\partial}{\partial x^{i'}} \right) = \frac{\partial}{\partial x^{i'}} \omega_j dx^j = \omega_j \frac{\partial x^j}{\partial x^{k'}} \delta_{i'}^{k'} = \frac{\partial x^j}{\partial x^{k'}} \omega_j \frac{\partial x^{k'}}{\partial x^{i'}} = \frac{\partial}{\partial x^{i'}} \omega_{k'} dx^{k'} \quad (3.10)$$

By comparing the coefficients one comes to the conclusion, that the components of the vectors and one-forms transform with the **Jacobian** of the coordinate change, also named **tangent map**

$$X^{i'} = \frac{\partial x^{i'}}{\partial x^j} X^j, \quad X = X^{i'} \frac{\partial}{\partial x^{i'}} \in \mathcal{X}(N) \quad (3.11)$$

$$\omega_{i'} = \frac{\partial x^j}{\partial x^{i'}} \omega_j, \quad \omega = \omega_{i'} dx^{i'} \in \mathcal{X}^*(N). \quad (3.12)$$

The tensorial product of r vectors $Y_a = Y^{i_a} \partial_{i_a} \in \mathcal{X}(M)$ and s one-forms $\Omega^b = \Omega_{j_b} dx^{j_b} \in \mathcal{X}^*(M)$ leads to an object:

$$T = Y_1 \otimes \dots \otimes Y_r \otimes \Omega^1 \otimes \dots \otimes \Omega^s = \quad (3.13)$$

$$= T^{i_1 \dots i_r}_{j_1 \dots j_s} \partial_{i_1} \otimes \dots \otimes \partial_{i_r} \otimes dx^{j_1} \otimes \dots \otimes dx^{j_s} \quad (3.14)$$

$$T^{i_1 \dots i_r}_{j_1 \dots j_s} = Y^{i_1} \cdot \dots \cdot Y^{i_r} \cdot \Omega_{j_1} \cdot \dots \cdot \Omega_{j_s}, \quad (3.15)$$

which is transformed component-wise by the tangential mapping of the coordinate change:

$$T^{i'_1 \dots i'_r}_{j'_1 \dots j'_s} = \frac{\partial x^{i'_1}}{\partial x^{k_1}} \cdot \dots \cdot \frac{\partial x^{i'_r}}{\partial x^{k_r}} \cdot \frac{\partial x^{l_1}}{\partial x^{j'_1}} \cdot \dots \cdot \frac{\partial x^{l_s}}{\partial x^{j'_s}} \cdot T^{k_1 \dots k_r}_{l_1 \dots l_s} \quad (3.16)$$

As a result of this transformation properties, $T \in \mathcal{T}_s^r(M)$ is called a **tensor field of type (r,s)** (contra-variant of rank r, covariant of rank s).

The numbers $T^{i_1 \dots i_r}_{j_1 \dots j_s}$ need not be a product of components of vectors, as it is done in equation (3.15). The $\partial_{i_1} \otimes \dots \otimes \partial_{i_r} \otimes dx^{j_1} \otimes \dots \otimes dx^{j_s}$ are then the $\dim(\mathcal{T}_s^r(M)) = n^{r+s}$ basis elements of the cartesian product $\mathcal{T}_s^r(M) = T_p M \times \dots \times T_p M \times T_p^* M \times \dots \times T_p^* M$ of the tensor space.

Given a linear transformation $A^i_{j'}$, tensors $T \in \mathcal{T}_s^r(M)$ transform in general by:

$$A(T) : T^{i'_1 \dots i'_r}_{j'_1 \dots j'_s} = A^{i'_1}_{k_1} \cdot \dots \cdot A^{i'_r}_{k_r} \cdot A^{l_1}_{j'_1} \cdot \dots \cdot A^{l_s}_{j'_s} \cdot T^{k_1 \dots k_r}_{l_1 \dots l_s} \quad (3.17)$$

Definition 3.3.1 (Tensor Field Contraction). Let $X_a = X^i{}_a \partial_i \in T_p(M)$ be s vectors and $\omega^b = \omega_{j_b} dx^{j_b} \in T_p^*(M)$ be r one-forms. A tensor field contraction is a mapping $\Pi_r^s(p) : T_p(M) \times \dots \times T_p(M) \times T_p^*(M) \times \dots \times T_p^*(M) \rightarrow \mathbb{R}$ which is defined by:

$$T(\omega^1, \dots, \omega^r, X_1, \dots, X_s) := \quad (3.18)$$

$$= T^{i_1 \dots i_r}{}_{j_1 \dots j_s} \cdot \omega^1(\partial_{i_1}) \cdot \dots \cdot \omega^r(\partial_{i_r}) \cdot \quad (3.19)$$

$$\cdot X_1(dx^{j_1}) \cdot \dots \cdot X_s(dx^{j_s}) = \quad (3.20)$$

$$= T^{i_1 \dots i_r}{}_{j_1 \dots j_s} \cdot \omega_{i_1} \cdot \dots \cdot \omega_{i_r} \cdot X^{j_1} \cdot \dots \cdot X^{j_s} \quad (3.21)$$

Applying an invertable, linear transformation $A^j{}_k A^i{}_{j'} = \delta^i_k$ to a tensor, one sees, that it's contraction is invariant under this transformation. This property makes tensors to well-defined objects.

3.4 Differential Forms

Definition 3.4.1 (Wedgebase Element). Let $(dx^{i_1}, \dots, dx^{i_r})$ be r different basis elements of $T_p^*(M)$, where $0 < i_1 < \dots < i_r \leq n$ are the indices of the space coordinates. The antisymmetric superposition of their tensor product is a wedgebase element of degree r :

$$dx^{i_1} \wedge \dots \wedge dx^{i_r} = \sum_{\sigma \in S_r} \text{sgn}(\sigma) dx^{\sigma(i_1)} \otimes \dots \otimes dx^{\sigma(i_r)} \in \Lambda^r, \quad (3.22)$$

where S_r is the set of all permutations of r objects and $\text{sgn}(\sigma)$ is the signature of the permutation σ .

The limited number of ordered indices of the space coordinates in $T_p^*(M)$ leads to a limited number of wedgebase elements:

$$\dim(\Lambda^r) = \binom{n}{r} = \frac{n!}{r!(n-r)!} \quad (3.23)$$

We find $dx^{i_1} \wedge \dots \wedge dx^{i_p} = \text{sgn}(\sigma) dx^{\sigma(i_1)} \wedge \dots \wedge dx^{\sigma(i_p)}$ for a permutation $\sigma \in S_r$.

Definition 3.4.2 (p-Form). Let $T \in \mathcal{T}_r(M)$ be a covariant tensor field. Contracting the tensor field coefficients with the wedge base elements leads to a total antisymmetric tensor field named **differential form of degree p** or **p-form**:

$$t_a = \frac{1}{r!} t_{i_1 \dots i_r} dx^{i_1} \wedge \dots \wedge dx^{i_r} \in \Lambda^r \quad (3.24)$$

A r -form can also be expanded as:

$$\omega = \frac{1}{r!} \omega_{i_1 \dots i_r} dx^{i_1} \wedge \dots \wedge dx^{i_r}, \quad (3.25)$$

where the expansion coefficients $\omega_{i_1 \dots i_r}$ are now total antisymmetric.

Definition 3.4.3 (Exterior Product). Let $\omega \in \Lambda^r$, $\eta \in \Lambda^q$, and $\omega_{i_1 \dots i_r}$, $\eta_{i_1 \dots i_q}$, be their expansion coefficients. The **exterior product** or **wedge product** is defined by:

$$\omega \wedge \eta = \frac{1}{r!q!} \omega_{i_1 \dots i_r} \eta_{i_{r+1} \dots i_{r+q}} dx^{i_1} \wedge \dots \wedge dx^{i_{r+q}} \in \Lambda^{r+q} \quad (3.26)$$

From this one can see, that it holds:

- $\omega \wedge \eta = (-1)^{p \cdot q} \eta \wedge \omega$
- \wedge is associative: $(\omega_1 \wedge \omega_2) \wedge \omega_3 = \omega_1 \wedge (\omega_2 \wedge \omega_3)$.

Definition 3.4.4 (Interior Product). Let $\omega \in \Lambda^r$ and $X \in T_p(M)$. The **interior product** $i_X \omega : \Lambda^r \rightarrow \Lambda^{r-1}$ is a contraction of the vector X with the first dual component of ω :

$$i_X \omega := \frac{1}{r!} \omega_{i_1 \dots i_r} (X(dx^{i_1})) \wedge dx^{i_2} \wedge \dots \wedge dx^{i_r} = \quad (3.27)$$

$$= \frac{1}{(r-1)!} X^{i_1} \omega_{i_1 \dots i_r} dx^{i_2} \wedge \dots \wedge dx^{i_r} \quad (3.28)$$

Definition 3.4.5 (Exterior Derivative). Let $\omega \in \Lambda^r$. The **exterior derivative** is a map $d : \Lambda^r \rightarrow \Lambda^{r+1}$ with the property:

$$d\omega = \frac{1}{r!} \left(\frac{\partial}{\partial x^i} \omega_{i_1 \dots i_r} \right) dx^i \wedge dx^{i_1} \wedge \dots \wedge dx^{i_r} \quad (3.29)$$

As a result of the permutability of partial derivatives on smooth functions and the antisymmetry of the wedgebase element $d \circ d = 0$ is always satisfied.

3.5 The Connection

3.5.1 Geometric interpretation

The connection can be introduced as a direction dependent linear transformation, which gives the change of a vector, which is moved on a manifold:

$$\zeta^i = \Gamma^i_{kj} \xi^j X^k \quad (3.30)$$

Here the Γ^i_{kj} are the **connection coefficients** or **Christoffel symbols**, ξ^j is the vector, which should be moved, ζ^i is the change of the vector and X^k specifies the direction of the movement.

The 'transformation law' (3.30) has the geometrical meaning that it glues together adjacent tangent spaces. Vectors in the tangent space $T_p(M)$, which are transported from a point $p \in M$ to the adjacent point $q \in M$ with tangent space $T_q(M)$ are in the general curved space affected by an infinitesimal change. The change of the vector by shifting it from p to q is characterized by the linear mapping $\Gamma(X)^i_j = \Gamma^i_{kj} X^k$, where $X = X^k \partial_k \in T_p(M)$ is the difference vector of p to q . One sees, that the change, which is assumed to be linear in the vector ξ and it's movement X is direction dependent.

3.5.2 Definition and properties

Definition 3.5.1 (Covariant Derivative). Let $T \in \mathcal{F}_s^r$, $\Lambda^1 \ni \Gamma \in \mathcal{F}_1^1$ and $c(t) \in \mathcal{F}_0^1$ be a smooth curve with $c(0) = p$ and $\dot{c}(0) = X$. The covariant derivative is the change of T along the X direction:

$$(\nabla_X T)_p := \left. \frac{d}{dt} [c(t). \Gamma[T(c(t))]] \right|_{t=0} \quad (3.31)$$

From this, one can see some important properties:

1. From the last comment of chapter 3.3, one concludes that ∇_X commutes with contractions.
2. ∇_X fulfills the Leibniz rule. This means: If $A \in \mathcal{F}_c^a$ and $B \in \mathcal{F}_d^b$ then $A \otimes B \in \mathcal{F}_{c+d}^{a+b}$ and:

$$\nabla_X(A \otimes B) = (\nabla_X A) \otimes B + A \otimes (\nabla_X B) \quad (3.32)$$

The most obvious consequences of (3.31) and (3.32) are:

3.

$$\nabla_X f = X.f, \quad f \in \mathcal{F}_0^0 \quad (3.33)$$

4.

$$\nabla_X Y = Y^i \nabla_X \partial_i + X.Y^i \cdot \partial_i, \quad X \in \mathcal{F}_0^1 \quad (3.34)$$

As a result of the property that $\nabla_X T$ is the change of T by walking along the curve $c(t)$ one also gets from reparametrisation:

5.

$$\nabla_{fX} T = f \nabla_X T, \quad f \in \mathbb{R} \quad (3.35)$$

Using the basis elements of $T_p(M)$ one gets:

$$\nabla_{\partial_k} \partial_j = \Gamma^i_{kj} \partial_i. \quad (3.36)$$

Transforming this basis to another basis and using the rules (3.34) and (3.35) of the covariant derivative, one sees that the Christoffel symbols transform not like a tensor does (see Eq. 3.16).

3.5.3 Component representation

Note, that the covariant derivative $\nabla_{\partial_i}(X^j\partial_j)$ is a generalization of the usual derivative $\partial_i(X^j\partial_j)$, which takes the curved space into account by introducing the linear transformation $\Gamma(X)^i_j$ as correction for the vector and tensor objects. For a vector $X = X^i\partial_i \in T_p(M)$ one can see this correction from (3.31) and (3.34): $\nabla_{\partial_j}(X^i\partial_i) = \partial_j(X^i\partial_i) + \Gamma^i_{jk}X^k\partial_i =: X^i_{;j}\partial_i$. Here, the component representation $X^i_{;j} = \partial_j X^i + \Gamma^i_{jk}X^k$ of the covariant derivative on vector fields was introduced, which can also be generalized to tensor fields of type (r,s) by using (3.32).

3.5.4 The generalized divergence

The generalized divergence of the components X^i of a vector field is now introduced by: $X^i_{;i} = X^i_{;i} + \Gamma^i_{ik}X^k$

Using some identities (see [8]) the divergence can be rewritten as: $X^i_{;i} = \frac{1}{\sqrt{g}}\partial_i(\sqrt{g}X^i)$.

In the same manner the divergence of symmetric $S \in \mathcal{T}_0^2$ and antisymmetric $T \in \mathcal{T}_0^2$ tensors of type $(2,0)$ can be written as $A^ki_{;i} = \frac{1}{\sqrt{g}}\partial_i(\sqrt{g}A^{ki})$ and $S^ki_{;i} = \frac{1}{\sqrt{g}}\partial_i(\sqrt{g}S^{ki}) + \Gamma^i_{kj}S^{kj}$.

3.6 The Metric

Definition 3.6.1 (Riemannian metric). Let $p \in M$ be a point of a manifold and $X, Y \in T_p(M)$. The Riemannian metric is a tensor $g \in \mathcal{T}_2^0(M)$ which is:

1. Symmetric: $\forall X, Y \in T_p(M) : g(X, Y) = g(Y, X)$
2. Non-degenerate: $\forall X \in T_p(M) : g(X, X) = 0 \Leftrightarrow X = 0$.

The metric tensor can be decomposed as: $g = g_{\mu\nu}dx^\mu \otimes dx^\nu$ Although it is named ‘metric’ the metric can be seen as mathematical² scalar product, which induces a mathematical norm $\|X\| := g(X, X)$ and on his part again induces (in flat spaces or infinitesimal distances) a mathematical metric $d(X, Y) := \|X - Y\|$, where $X, Y \in T_p(M)$. So the metric can be used for measure distances and length-scales.

The metric coefficients of the Euclidean space, we are living in is: $g_{ij} = \text{diag}(1, 1, 1)$.
The physical Minkowski space has a pseudo³-Euclidean metric: $\eta_{\mu\nu} := \text{diag}(-1, 1, 1, 1)$.

As a result, distances $\|X\|$ in the Minkowski space can be:

- Timelike, if $\|X\| < 0$
- Spacelike, if $\|X\| > 0$
- Null, if $\|X\| = 0$ (X is lying at the light cone).

In **local coordinates**, which are introduced in the sections 3.1 and 3.2 and whose basis elements are $\partial_\mu \in T_p(M)$ and $dx^\mu \in T_p^*(M)$ the metric is in general not Euclidean or Minkowskian.

One may change to the coordinates of the **orthonormal frame**, whose basis elements are denoted as $e_\mu \in T_p(M)$ and $\theta^\mu \in T_p^*(M)$. In the orthonormal frame the metric always takes the Minkowskian form: $g_{\mu\nu} = \eta_{\mu\nu} = \text{diag}(-1, 1, 1, 1)$. The metric is then: $g = \eta_{\mu\nu}\theta^\mu \otimes \theta^\nu$

For denoting the connection coefficients in the orthonormal frame we use ω :

$$\nabla_{e_k} e_j = \omega^i_{kj} e_i, \quad \omega^i_j = \omega^i_{kj} \theta^k \quad (3.37)$$

instead of Γ^i_{kj} .

² Mathematical means in terms of the usual (functional) analysis.

³ Pseudo stands for the -1 in the metric.

3.7 Torsion and Curvature

The Torsion and Curvature are defined as tensor fields of higher rank:

$$T(X, Y) := \nabla_X Y - \nabla_Y X - [X, Y] \quad (3.38)$$

$$R(X, Y)Z := \nabla_X(\nabla_Y Z) - \nabla_Y(\nabla_X Z) - \nabla_{[X, Y]}Z, \quad (3.39)$$

where $[X, Y]f := X.(Y.f) - Y.(X.f)$ is the commutator. As a result of the property $T(X, Y) = -T(Y, X)$ and $R(X, Y) = -R(Y, X)$, we see that $T, R \in \Lambda^2$ for the torsion and the curvature.

Contracting by using the basis vectors one obtains the **torsion tensor** and the **curvature tensor** (also called **Riemann Tensor**):

$$T(\partial_j, \partial_k).dx^i := T^i_{jk} \quad (3.40)$$

$$(R(\partial_k, \partial_l)\partial_j).dx^i := R^i_{jkl}, \quad (3.41)$$

from which one can see, that $T \in \mathcal{T}_2^1(M)$ and $R \in \mathcal{T}_3^1(M)$.

The Riemann tensor fulfills $R_{ijkl} = R_{klij}$ and the first Bianchi identity (3.45). Together with the antisymmetry of the curvature the number of independent components of the Riemann tensor reduces to $F(n) = \frac{1}{12}n^2(n^2 - 1)$, which is $F(4) = 20$ in the four-dimensional space.

One obtains the **Ricci tensor** by contracting the first and third index of the Riemann tensor: $R_{ij} := R^k_{ikj}$.⁴ A further contraction of the Ricci tensor leads to the **scalar curvature**: $R := R^i_i$.

3.8 Resulting relations

3.8.1 Identities

One sees by direct calculation, that the **Jacobi identity** holds:

$$\sum_{cyclic} [X, [Y, Z]] = 0. \quad (3.42)$$

Using this identity and (3.32) one can also verify the two following relations by a straightforward calculation of the most left-hand term:

- First Bianchi identity:

$$\sum_{cyclic} (R(X, Y)Z) = \sum_{cyclic} (T(T(X, Y), Z) + (\nabla_X T)(Y, Z)) \quad (3.43)$$

- Second Bianchi identity:

$$\sum_{cyclic} ((\nabla_X R)(Y, Z) + R(T(X, Y), Z)) = 0. \quad (3.44)$$

If the geometry is given by the Levi-Civita connection ($T(X, Y) = 0$) the Bianchi identities reduce to:

$$\sum_{cyclic} (R(X, Y)Z) = 0 \quad (3.45)$$

$$\sum_{cyclic} ((\nabla_X R)(Y, Z)) = 0. \quad (3.46)$$

⁴ As a result of the antisymmetry, there is only one way for contracting the indices which makes sense.

3.8.2 The Levi-Civita connection

Definition 3.8.1 (Levi-Civita connection). The Levi-Civita connection is a connection ∇ , which has the properties:

1. The connection is metric: $\nabla_X g = 0, \forall X \in T_p(M)$
2. The torsion vanishes: $T(X, Y) = 0, \forall X, Y \in T_p(M)$

Annotations:

The property $\nabla_X g = 0$ has the interpretation, that the connection preserves the inner product, given by $g(Y, Z)$. By using the first two properties of the covariant derivative it can also be written as:

$$\nabla_X(g)(Y, Z) = (X \cdot g)(Y, Z) - g(\nabla_X Y, Z) - g(Y, \nabla_X Z), \quad (3.47)$$

which is also known as Ricci identity. In components the Ricci identity also reads:

$$dg_{ij} = \Gamma_{ij} + \Gamma_{ji}. \quad (3.48)$$

The torsion measures the lowest order deviation of a closed path. If one tries to move on an infinitesimal rhombus (spanned by X and Y) by taking the geodesics along the directions X and Y the lowest order deviation is given by $T(X, Y)$. A detailed discussion is given in §92 of [14].

Inserting (3.38) with $T(X, Y) = 0$ into (3.47), performing a cyclic summation of the terms and using the basis elements ∂_i as vectors one obtains an expression for the Christoffel symbols, which only depend on the given metric:

$$\Gamma_{jk}^i = \frac{1}{2} g^{il} (g_{lj,k} + g_{lk,j} - g_{jk,l}). \quad (3.49)$$

One ends up at the same equation by the principle of the stationary action applied to the line-element $d\tau = \sqrt{g_{\mu\nu} \frac{\partial x^\mu}{\partial \tau} \frac{\partial x^\nu}{\partial \tau}} d\tau$. So it stands to reason, that the Levi-Civita connection is an especially ‘natural’ one.

3.9 The Cartan Structure Equations

The torsion and the curvature also depend on the connection. This dependence can be calculated in an orthonormal frame and results in the Cartan structure equations:

$$\Theta^i = d\theta^i + \omega^i_j \wedge \theta^j \quad (3.50)$$

$$\Omega^i_j = d\omega^i_j + d\omega^i_k \wedge \omega^k_j \quad (3.51)$$

, where the **torsion forms** Θ^i and **curvature forms** Ω^i_j fulfill the relations:

$$T(X, Y) = \Theta^i(X, Y)e_i \quad \Theta^i = \frac{1}{2} T^i_{kl} \theta^k \wedge \theta^l \quad (3.52)$$

$$R(X, Y)e_j = \Omega^i_j(X, Y)e_i \quad \Omega^i_j = \frac{1}{2} R^i_{jkl} \theta^k \wedge \theta^l \quad (3.53)$$

3.10 Conformal Transformations

Definition 3.10.1 (Isometry). A mapping $x'(x) : M \rightarrow N$ is an isometry, if it preserves the metric:

$$\frac{\partial x'^\alpha}{\partial x^\mu} \frac{\partial x'^\beta}{\partial x^\nu} g_{\alpha\beta}(x'(x)) = g_{\mu\nu}(x) \quad (3.54)$$

Every pseudo-Riemannian manifold which is isometric / locally isometric to (\mathbb{R}^4, η) is said to be **flat** / **locally flat**, where η is the Minkowski metric.

Definition 3.10.2 (Conformal transformation). A mapping $x'(x) : M \rightarrow N$ is a conformal transformation, if it preserves the metric up to a scale:

$$\frac{\partial x'^\alpha}{\partial x^\mu} \frac{\partial x'^\beta}{\partial x^\nu} g_{\alpha\beta}(x'(x)) = e^{2\sigma(x)} g_{\mu\nu}(x), \quad (3.55)$$

where $\Omega(x) = e^{2\sigma(x)}$ is called **conformal factor**.

It is an important property that the angle of two vectors is preserved under a conformal transformation. Every pseudo-Riemannian manifold whose metric can be conformally transformed to (\mathbb{R}^4, η) is said to be **conformally flat**. The **Weyl tensor** given by

$$C_{\kappa\lambda\mu\nu} = R_{\kappa\lambda\mu\nu} + \frac{1}{m-2}(R_{\kappa\mu}g_{\lambda\nu} - R_{\lambda\mu}g_{\kappa\nu} + \tag{3.56}$$

$$+ R_{\lambda\nu}g_{\kappa\mu} - R_{\kappa\nu}g_{\lambda\mu}) \frac{R}{(m-2)(m-1)}(g_{\kappa\mu}g_{\lambda\nu} - g_{\kappa\nu}g_{\lambda\mu}) \tag{3.57}$$

is invariant under conformal transformations: $C'_{\kappa\lambda\mu\nu} = e^{2\sigma(x)}C_{\kappa\lambda\mu\nu}$. As a result the Weyl tensor always vanishes in conformally flat spaces, because $C_{\kappa\lambda\mu\nu} = 0$ in flat spaces.

4 The Homogeneous Universe

4.1 Einstein's Field Equations

In Special Relativity the energy-stress tensor of a fluid

$$T^{\mu\nu} = (\rho + p)u^\mu u^\nu + p g^{\mu\nu} \quad (4.1)$$

has a vanishing divergence: $T^{\mu\nu}_{;\nu} = 0$. In the curved space of General Relativity the generalized divergence should also vanish: $T^{\mu\nu}_{;\nu} = 0$. The combination

$$G_{\mu\nu} = R_{\mu\nu} - \frac{R}{2}g_{\mu\nu} \quad (4.2)$$

of geometry related tensors of rank two is called Einstein tensor. Due to the second Bianchi identity (3.46) it is divergence free too. For this reason it makes sense, that the Einstein tensor couples directly to the energy-stress tensor:

$$G_{\mu\nu} = 8\pi G T_{\mu\nu}, \quad (4.3)$$

where G is the gravitational constant. These are **Einstein's field equations**.

The Hilbert action $S_H = R\sqrt{-g}$ yields also to (4.3) under the variation with respect to the metric, where $T_{\mu\nu} = 2\frac{1}{\sqrt{-g}}\frac{\delta S_m}{\delta g^{\mu\nu}}$ has to be identified for some matter action S_m . So like in subsection 3.8.2 it stands to reason, that Einstein's field equations are especially 'natural' ones.

4.2 Using symmetries

The following derivation of the FRW model is mainly taken from [9], [10], [3].

Assuming homogeneity and isotropy and demanding the introduction of a cosmic time t , for which $\nabla_u u = 0$ holds one makes the following ansatz for the space-time metric of the universe:

$$ds^2 = -dt^2 + a^2(t)\gamma_{ij}dx^i dx^j = dt^2 + a^2(t)d\sigma_{(3)}^2, \quad (4.4)$$

where the space-like part can be denoted in the short-hand notation $d\sigma_{(3)}^2$. Here, one can also introduce the conformal time η by $dt = d\eta a(t)$, for which one gets the conformal metric:

$$ds^2 = a^2(t)(-d\eta^2 + d\sigma_{(3)}^2). \quad (4.5)$$

The sectional curvature has to be introduced for the next consideration of Schur's lemma: For every plane E in the tangential space $T_p M$ of a point p is $K_p(E) := R(e_1, e_2, e_1, e_2)$ the **sectional curvature**, where $e_1, e_2 \in T_p M$ are the basis elements of E .

Schur's lemma states, that if $K_p(E)$ is independent of E and p (isotropy), then the assumed pseudo-Riemannian manifold M is homogeneous and has a constant curvature. The curvature tensor of a constant curvature is given by:

$$R_{abcd} = K(g_{ac}g_{bd} - g_{ad}g_{bc}) \quad (4.6)$$

By using (3.53) one obtains the curvature form of constant curvature:

$$\Theta_{ab} = K \theta_a \wedge \theta_b \quad (4.7)$$

From (4.6) one can calculate the Ricci tensor, the scalar curvature and read off the Weyl tensor:

$$R_{bd} = g^{ac}R_{abcd} = K(n-1)g_{bd} \quad (4.8)$$

$$R = g^{bd}R_{bd} = Kn(n-1) \quad (4.9)$$

$$C_{abcd} = 0 \quad (4.10)$$

One concludes that the space of constant curvature is conformally flat. So according to (3.55) one can always change the coordinates to those, where the space-like part of the metric is of the form $e^{2\sigma(x)}g_{ij}$, where g_{ij} is the euclidean metric. For easier calculation this can also be rewritten as:

$$d\sigma_{(3)}^2 = \frac{1}{\Psi^2(x)} \sum_i dx^i \otimes dx^i \quad (4.11)$$

$$ds^2 = -dt^2 + \frac{a^2(t)}{\Psi^2(x)} \sum_i dx^i \otimes dx^i, \quad (4.12)$$

where we can again change into the orthonormal frame:

$$\theta^0 = dt \quad , \quad \theta^i = \frac{a(t)}{\Psi(x)} dx^i \quad (4.13)$$

$$ds^2 = \eta_{\mu\nu} \theta^\mu \otimes \theta^\nu. \quad (4.14)$$

In order to get an expression for the function $\Psi(x)$ the curvature will be calculated by using Cartan's structure equations. First, the Levi-Civita connection is obtained by using the first Cartan's structure equation with vanishing torsion $\Theta^i = 0$ and an antisymmetric connection of the orthonormal frame $dg_{ij} = 0 = \omega_{ij} + \omega_{ji}$ (see Eq. 3.48):

$$d\Theta^0 = 0 \quad (4.15)$$

$$d\Theta^i = \frac{a_{,0}}{\Psi} dx^0 \wedge dx^i + a(\Psi^{-1})_{,k} dx^k \wedge dx^i = \quad (4.16)$$

$$= \frac{a_{,0}}{a} \theta^0 \wedge \theta^i - \frac{\Psi_{,k}}{a} \theta^k \wedge \theta^i = -\omega^i_0 \wedge \theta^0 - \omega^i_k \wedge \theta^k = \quad (4.17)$$

$$= \omega^i_{j0} \theta^0 \wedge \theta^j + \omega^i_{jk} \theta^k \wedge \theta^j = \quad (4.18)$$

$$= \omega^i_j{}^{il} \eta_{l0} \theta^0 \wedge \theta^j + \omega^i_j{}^{ik} \eta_{kl} \theta^l \wedge \theta^j = \quad (4.19)$$

$$= -\omega^i_0 \theta^0 \wedge \theta^j + \omega^i_k \theta^k \wedge \theta^j, \quad (4.20)$$

From this one can read off the non-vanishing connection coefficients:

$$\omega_j^{i0} = -\omega_j^{0i} = -\delta_j^i \frac{\dot{a}}{a} \quad (4.21)$$

$$\omega_j^{ik} = -\omega_j^{ki} = -\delta_j^i \frac{\Psi_{,k}}{a} + \delta_j^k \frac{\Psi_{,i}}{a}, \quad (4.22)$$

where $\delta^\mu_\nu = \eta^{\mu\lambda} \eta_{\lambda\nu} = \text{diag}(1, 1, 1, 1)$. The connection one-forms are then:

$$\omega^{i0} = -\omega^{0i} = -\frac{\dot{a}}{a} \theta^i \quad (4.23)$$

$$\omega^{ik} = -\omega^{ki} = \frac{\Psi_{,i}}{a} \theta^k - \frac{\Psi_{,k}}{a} \theta^i, \quad (4.24)$$

The space-like curvature form can now be calculated by using Cartan's second structure equation (3.53):

$$\Omega_{ij} = d\omega_{ij} + \omega_i^m \wedge \omega_{mj} = \quad (4.25)$$

$$= -\Psi \Psi_{,jm} \theta^m \wedge \theta^i + \Psi \Psi_{,im} \theta^m \wedge \theta_j - \Psi_{,m} \Psi^m \theta_i \wedge \theta_j \quad (4.26)$$

This space-like curvature should have the form of the constant curvature form (4.7). That is to say

$$K = \Psi(\Psi_{,mj} + \Psi_{,mi}) - \Psi_{,m} \Psi^m \quad (4.27)$$

and so $\Psi_{,mj} = 0$, $\forall m \neq j$ must hold. The term $\Psi_{,mj} + \Psi_{,mi}$ must also be independent of i and j , because the rest does so. Now one can argue, that Ψ must be of the form:

$$\Psi = \frac{K\rho^2}{4} + 1 \quad , \quad \rho^2 := \sum_i x_i^2. \quad (4.28)$$

The space-like connection simplifies to:

$$\omega^{ik} = -\omega^{ki} = \frac{K}{2a} x^i \theta^k - \frac{K}{2a} x^k \theta^i. \quad (4.29)$$

4.3 Friedmann-Robertson-Walker space-time

Beforehand there are four explanatory notes:

1. In the following the polar differential of the 2-sphere is shortened by $d\Omega^2 = d\theta^2 + \sin^2\theta d\phi^2$.
2. In this subsection it can be realized, that the curvature K can be normalized to 1, 0, -1. To do so, the space-like extensions have to be rescaled.
3. The scale factor a can be rescaled to a fixed value at a specific time, where usually the scale factor today is chosen to be one: $a(t_0) = 1$.
4. Instead of the usual time differential dt one uses very often the conformal time differential $d\tau = \frac{dt}{a}$ in cosmological perturbation theory. From this it holds for a function $f(t)$:

$$\dot{f}(t) = \frac{df}{dt} = \frac{df}{d\tau} \frac{d\tau}{dt} = \frac{df}{d\tau} \frac{1}{a}. \quad (4.30)$$

The metric of the homogeneous and isotropic densed universe can be expressed in three ways, which are mapped via

$$r = \frac{\rho}{1 + K\rho^2/4}, \quad r = \begin{cases} = \sin(\chi) : & K = 1 \\ = \chi : & K = 0 \\ = \sinh(\chi) : & K = -1 \end{cases} \quad (4.31)$$

to each other:

1. The conformal metric

$$ds^2 = -dt^2 + \frac{a^2(t)}{(1 + K\rho^2/4)^2} (d\rho^2 + \rho^2 d\Omega^2) \quad (4.32)$$

This metric results from the considerations of the above section.

2. Friedman Robertson Walker metric

$$ds^2 = -dt^2 + a^2 \left(\frac{dr^2}{1 - Kr^2} + r^2 d\Omega^2 \right) \quad (4.33)$$

This is the standard textbook version of the Friedman Robertson Walker metric.

3. Embedded metric

$$K = 1 : \quad ds^2 = -dt^2 + a^2 (d\chi^2 + \sin^2(\chi)d\Omega^2) \quad (4.34)$$

$$K = 0 : \quad ds^2 = -dt^2 + a^2 (d\chi^2 + \chi^2 d\Omega^2) \quad (4.35)$$

$$K = -1 : \quad ds^2 = -dt^2 + a^2 (d\chi^2 + \sinh^2(\chi)d\Omega^2) \quad (4.36)$$

This metric is the induced metric of a 3-sphere ($K = 1$) / flat space ($K = 0$) / hyperboloid of one sheet ($K = -1$). So the space of constant curvature and hence the space-like, averaged part of the universe can be embedded as a three-dimensional hyper-surface in the four-dimensional space. (I like embeddings!)

In flat spaces ($K = 0$) the metric 4.33 gets by expressing it in conformal time:

$$ds^2 = a^2 (-d\tau^2 + dr^2 + r^2 d\Omega^2) \quad (4.37)$$

4.4 Scale factor and Redshift

For simplicity the flat space (4.37) will now be discussed. The considerations can also be extended to (4.34) and (4.36). The space-time metric suggests, that there are comoving coordinates \vec{r} , which are blown up to the real physical coordinates \vec{x} by a scale factor $a(t)$:

$$\vec{x}(t) = a(t)\vec{r}, \quad (4.38)$$

where a is set to $a(t_0) = 1$ at the present time t_0 . The radial distance and the radial velocity is then:

$$R = |x(t)| = a(t)|\vec{r}| = a(t)r \quad (4.39)$$

$$v = \dot{R} = \dot{a}(t)|\vec{r}|. \quad (4.40)$$

Both are related by Hubble's Law:

$$v = HR \quad \Rightarrow \quad H = \frac{\dot{a}}{a}, \quad (4.41)$$

In conformal time Hubble's Law gets modified:

$$\mathcal{H} := \frac{da}{d\eta} \frac{1}{a} = \frac{da}{dt} = Ha, \quad (4.42)$$

The expansion today is given by the **Hubble constant**:

$$H_0 := H(t_0) = 70.1 \pm 1.3 \frac{km}{s Mpc}. \quad (4.43)$$

This value is obtained from [21], including data from WMAP, SN 1a and BAO.

The deceleration at large distances $\dot{v} = -AR$ is also important for cosmology, where $A = -\ddot{a}/a$ has to be rescaled by H_0^2 , to get a dimensionless quantity in (4.79):

$$q_0 := -\frac{A}{H(t)^2} = -\frac{\ddot{a}a}{\dot{a}^2}. \quad (4.44)$$

The comoving distance gets stretched. The wavelength (and its frequency) of an emitted photon increases and it gets red-shifted while it is traveling through the universe until absorption:

$$\frac{\nu_e}{\nu_0} = \frac{\lambda_0}{\lambda_e} = \frac{\Delta r a(t_0)}{\Delta r a(t_e)} = \frac{a(t_0)}{a(t_e)} \quad (4.45)$$

The redshift itself is defined by:

$$z := \frac{\nu_e - \nu_0}{\nu_0} = \frac{\lambda_0 - \lambda_e}{\lambda_e} = \frac{a(t_0)}{a(t_e)} - 1 \quad \Rightarrow \quad 1 + z = \frac{a(t_0)}{a(t_e)} \quad (4.46)$$

From the frequency shift one also concludes that the proper time of an observed event is increased:

$$\frac{\Delta t_0}{\Delta t_e} = \frac{\nu_e}{\nu_0} = \frac{a(t_0)}{a(t_e)} \quad (4.47)$$

On small distances the velocities given by Hubble's law are small. The Doppler shift of a photon with wavelength $\lambda = cT$ (T = oscillation period) can then be approximated by $\Delta\lambda = vT \ll \lambda$. From (4.46) one obtains:

$$z = \frac{\Delta\lambda}{\lambda_e} \approx \frac{\Delta\lambda}{\lambda} = \frac{vT}{cT} = \frac{v}{c} \quad (4.48)$$

If v reaches c and so z reaches 1 this approximation is no longer correct, which corresponds to a length scale called **Hubble radius**:

$$R_H(t) = \frac{c}{H(t)}, \quad R_H(t_{today}) = \frac{c}{H_0} = 4.28 Gpc \quad (4.49)$$

4.5 Distance and angular width

The energy flux F , which is observed in a time interval Δt_0 from a distant object with the luminosity L during the interval Δt_e would be:

$$F \Delta t_0 = \frac{L \Delta t_e}{4\pi R(t_0)^2} \frac{a(t_e)}{a(t_0)} \quad (4.50)$$

with respect to the redshift (4.45). Rewriting it

$$F = \frac{L}{4\pi r_e^2 a_0^2 (1+z)^2} \quad (4.51)$$

one can identify the **luminosity distance**:

$$d_L = r_e a(t_0) (1+z), \quad (4.52)$$

which is related by the **distance modulus** $m - M = 5 \log(d_L / pc) - 5$ to cosmic observations.

The comoving radius r_e of the past light emission is given by the metric 4.33:

$$r_e = - \int_{r_e}^0 dr = \int_{t_e}^{t_0} \frac{cdt}{a(t)} \underset{z \ll 1}{=} \int_{t_e}^{t_0} cdt = c(t_0 - t_e), \quad (4.53)$$

where c was inserted to recover the distance, which was traveled by light during the time dt and a further approximation for $z \ll 1$ was made.

By performing a Taylor expansion of $1+z$:

$$1+z = \frac{a(t_0)}{a(t_e)} \approx a(t_0) \left(1 - \frac{\dot{a}(t_e)}{a^2(t_e)} (t_e - t_0) + O(t^2) \right) \approx 1 + H_0(t_0 - t_e), \quad (4.54)$$

and inserting the result $z = H_0(t_0 - t_e)$ into (4.53) one ends up in an approximation for the luminosity distance for small redshifts $z \ll 1$:

$$d_L = r_e a_0 (1+z) \approx c(t_0 - t_e) = \frac{cz}{H_0} = R_H z. \quad (4.55)$$

The the once observed angular diameter D of an extension is:

$$D(t_e) = a(t_e) r_e \sin(\Delta\theta) \approx a(t_e) r_e \Delta\theta = \frac{a(t_0) r_e \Delta\theta}{1+z} = \frac{d_L \Delta\theta}{(1+z)^2} = d_A \Delta\theta, \quad (4.56)$$

where the **angular diameter distance** $d_A := a(t_e) r_e = d_L / (1+z)^2$ was introduced. For small z the distance measures do not differ from each other.

However for $z \geq 1$ one has to integrate the third term of equation 4.53, for obtaining the distances in z -dependence. There exist some fitting formulas for the distances. Using eq. (1) of [24], one obtains at the redshift of recombination $z_{rec} = 1133.862$ by using the cosmological parameters mentioned in section 6.2:

$$d_L = 3792 \cdot R_H = 1.620 \cdot 10^7 Mpc \quad (4.57)$$

$$d_A = 0.00294 \cdot R_H = 12.58 \cdot Mpc \quad (4.58)$$

Especially the comoving size of an object seen during recombination with angle $\Delta\theta$ is today:

$$D(t_0) = D(t_e) \frac{a(t_0)}{a(t_e)} = D(t_e) \cdot (1+z) = (1+z) d_A \Delta\theta = 3.342 \cdot R_H \Delta\theta \Leftrightarrow \Delta\theta = \frac{0.2992 \cdot D(t_0)}{R_H}. \quad (4.59)$$

4.6 The Friedmann Equations

Summing over the time- and space-like connections one obtains:

$$\Omega^0_i = \frac{\ddot{a}}{a} \theta^0 \wedge \theta^i \quad (4.60)$$

$$\Omega^i_j = \frac{k + \dot{a}^2}{a^2} \theta^i \wedge \theta^j. \quad (4.61)$$

One ends up at the **Friedmann equations** by reading off the components of the curvature tensor, contracting them to the Ricci tensor and the scalar curvature, constructing the Einstein tensor and putting it into Einstein's field equations (4.3):

$$G_{00} = 3 \frac{K + \dot{a}^2}{a^2} = 8\pi G \rho \quad (4.62)$$

$$G_{11} = G_{22} = G_{33} = -2 \frac{\ddot{a}}{a} - \frac{K + \dot{a}^2}{a^2} = 8\pi G p \quad (4.63)$$

where the energy-stress tensor of the comoving rest frame of the fluid ($u^\mu = (1, 0, 0, 0)^T$, $T^{\mu\nu} = \text{diag}(\rho, p, p, p)$) has been used. The other off-diagonal terms of Einstein's field equation vanish.

Inserting (4.62) into (4.63) yields to the **acceleration equation**:

$$\ddot{a} = -\frac{4\pi G}{3}(\rho + 3p)a \quad (4.64)$$

4.6.1 Density evolution

Multiplying (4.62) by a^3 , differentiating with respect to t and inserting (4.63) at the left hand side one obtains:

$$\frac{d}{dt}(\rho a^3) = -p \frac{d}{dt}(a^3) \Rightarrow \dot{\rho} = -3(\rho + p) \frac{\dot{a}}{a}, \quad (4.65)$$

which is called cosmic energy conservation, because it is equivalent to the first law of thermodynamics:

$$dU = d(\rho V) = d(\rho a^3) = dQ + dW = dW = -p dV = -p d a^3 \quad (4.66)$$

Using (4.65) one can obtain how the density of different matter types changes with an increasing universe. The matter types only differ by their ratio of pressure and density $p/\rho = \omega$. Integrating (4.65) by using ω one ends up with:

$$\rho(t) = \rho(t_0) \frac{a(t_0)^{3(1+\omega)}}{a(t)^{3(1+\omega)}} = \rho(t_0)(1+z)^{3(1+\omega)}. \quad (4.67)$$

The standard matter types are:

Dust The non-relativistic matter has no pressure $p = 0$. (4.67) reads then:

$$\rho_M(t) = \rho_M(t_0) \frac{a(t_0)^3}{a(t)^3} = \rho_M(t_0)(1+z)^3, \quad (4.68)$$

as it should be and is well known from everyday live too.

Radiation For the relativistic matter we have $p = \rho/3$. (4.67) reads then:

$$\rho_R(t) = \rho_R(t_0) \frac{a(t_0)^4}{a(t)^4} = \rho_R(t_0)(1+z)^4. \quad (4.69)$$

Vacuum The physical vacuum has a negative pressure: $p = -\rho$. (4.67) yields:

$$\rho_\Lambda(t) = \rho_\Lambda(t_0) = \rho_0(1+z)^0 \quad (4.70)$$

The physical vacuum remains always constant! Some theories behind the standard model predict, that ω does not remain constant at -1 for vacuums. In that case one has to go back and use (4.65) or (4.67).

Curvature The curvature itself is no matter, but it behaves like matter in the Friedmann equation (4.62):

$$\rho_K(t) = \rho_K(t_0) \frac{a(t_0)^2}{a(t)^2} = \rho_K(t_0)(1+z)^2. \quad (4.71)$$

The "pressure" one of this curvature density would then be: $\omega = -1/3$.

4.7 Density Parameters

The overall density of the universe has contributions from the densities mentioned above:

$$\rho(t) = \rho_M(1+z)^3 + \rho_R(1+z)^4 + \rho_\Lambda + \rho_K(1+z)^2 + \dots? \quad (4.72)$$

The Friedmann equation (4.62) can now be made dimensionless by dividing it through H_0^2 . Together with the overall density it reads:

$$\frac{H(t)^2}{H_0^2} = \frac{8\pi G}{3H_0^2} \left(\rho_M(1+z)^3 + \rho_R(1+z)^4 + \rho_\Lambda + \rho_K(1+z)^2 \right) \quad (4.73)$$

The inverse of the foremost factor of the right hand side is defined as the **critical density**:

$$\rho_{crit} := \frac{3H_0^2}{8\pi G}, \quad (4.74)$$

which fulfills $\rho_{crit} = \rho(t_0)$ today. The densities of the different matter types can then be made to the dimensionless density parameters:

$$\Omega_M := \frac{\rho_M}{\rho_{crit}}, \quad \Omega_R := \frac{\rho_R}{\rho_{crit}}, \quad \Omega_\Lambda := \frac{\rho_\Lambda}{\rho_{crit}}, \quad \Omega_K := \frac{\rho_K}{\rho_{crit}}, \quad (4.75)$$

which fulfill today:

$$1 = \Omega_M + \Omega_R + \Omega_\Lambda + \Omega_K. \quad (4.76)$$

One ends up with the reduced form of the Friedmann equation:

$$H(t)^2 = H_0^2 \left(\Omega_M(1+z)^3 + \Omega_R(1+z)^4 + \Omega_\Lambda + \Omega_K(1+z)^2 \right) \quad (4.77)$$

From (4.64) one can also calculate:

$$q_0 = \frac{1}{2} \frac{\Omega_M(1+z)^3 + 2\Omega_R(1+z)^4 - 2\Omega_\Lambda}{\Omega_M(1+z)^3 + \Omega_R(1+z)^4 + \Omega_\Lambda + \Omega_K(1+z)^2}, \quad (4.78)$$

which reduces to:

$$q_0 = \frac{1}{2} (\Omega_M + 2\Omega_R - 2\Omega_\Lambda) \quad (4.79)$$

at the present time. The Friedman equation can be integrated for only one matter species, to get an analytical expansion law in time-dependence of one matter species:

Species	Matter	Radiation	Curvature	Vacuum
$\omega =$	0	$\frac{1}{3}$	$-\frac{1}{3}$	-1
Time $a(t) =$	$\left(\frac{3}{2}H_0(t+t_0) + a_0^{\frac{3}{2}} \right)^{\frac{2}{3}}$	$\left(2H_0(t+t_0) + a_0^2 \right)^{\frac{1}{2}}$	$H_0(t+t_0) + a_0$	$a_0 e^{H_0(t+t_0)}$
Conformal Time $a(\tau) =$	$\left(\frac{1}{2}H_0(\tau - \tau_0) + a_0^{\frac{1}{2}} \right)^2$	$H_0(\tau - \tau_0) + a_0$	$a_0 e^{H_0(\tau - \tau_0)}$	$\frac{1}{a_0 - (H_0(\tau - \tau_0))}$

Table 4.1: Scale factor dependence for one matter species

Note, that the time $t_0 = \frac{1}{H_0}$, at which $a(t_0) = 1$ holds is not the exact age of the universe, if the today's Hubble constant H_0 is used. Due to lucky circumstances the universe is currently in a stage, at which $t_0 \approx \frac{1}{H_0} = \frac{R_H}{c} = 4.41 \cdot 10^{17} s = 13.97 G_y$ approximately holds.

4.7.1 Values of the density parameters

There are several methods for obtaining the density parameters:

1. **Supernovae of type 1A:** This method measures the redshift and distance of distant comoving objects and fits the data through the Friedmann equation (4.77). The distant comoving objects are Supernovae 1a (SN 1a) in astronomy (lhs of fig. 4.1).
2. **The cosmic microwave background radiation:** The small temperature fluctuations ΔT of the CMB can be decomposed into spherical harmonics and their amplitudes in dependence of l are investigated:

$$a_{lm} = \int \Delta T(\Theta, \Phi) Y_{lm}(\Theta, \Phi) d\Omega \quad , \quad \delta T(l) = \langle |a_{lm}|^2 \rangle = \sum_{m=-l}^{m=l} |a_{lm}|^2 \quad , \quad (4.80)$$

which is shown in the right-hand side figure 4.1. The first peak of this power spectrum is very sensitive to the curvature density Ω_K , where the second and third peaks are sensitive to the contributions of the baryon- and dark matter density Ω_b, Ω_c .

3. **Baryonic acoustic oscillations:** In the early universe the density fluctuations of dark matter generate a gravitational potential, in which the baryonic matter performs acoustic oscillations. These oscillations depend on the density parameters too. Today they are manifested in the galaxy power spectrum.
4. **Clustering** This method is a direct measurement of the matter density. It is done by obtaining the velocity distribution of galaxy clusters, from which the whole gravitating mass can be determined. Using this method one obtains $\Omega_M \approx 0.3$

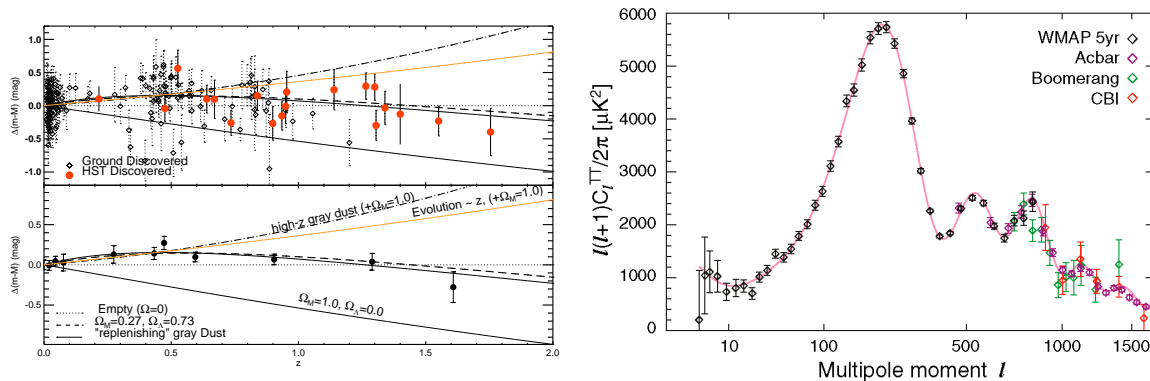


Figure 4.1: Left: Redshift of SN 1a, Right: Spherical harmonic contributions of the CMB

The left figure shows the distance modulus in dependence of the redshift. The dots are supernovae of type 1a. The redshift dependence of some density parameters is also plotted. The universe with $\Omega_M = 0.27$ and $\Omega_\Lambda = 0.73$ is preferred. (Adapted from [22], Fig. 7)

On the right, the amplitude $\delta T(l)$ of the spherical harmonics (4.80) is plotted over the multipole moment l . The Acbar, Boomerang and CBI data are radio astronomy and the WMAP data comes from a satellite. The maxima of the amplitudes get changed in their intensity and location, if Ω_M and Ω_Λ are modified. Thus one can fit the density parameters to the CMB. (The figure is taken from the WMAP homepage.)

The density parameters are usually mapped in the fundamental plane of cosmology (figure 4.2).

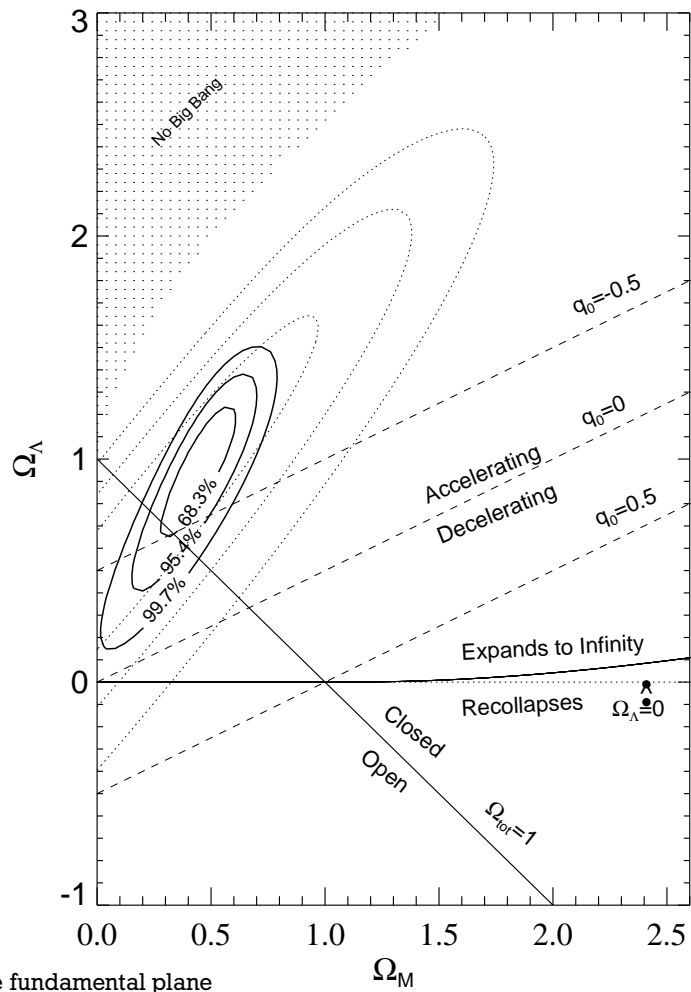


Figure 4.2: SN Ia data at the fundamental plane

At the fundamental plane the parameters Ω_M and Ω_Λ can vary. Ω_K varies also indirectly because of (4.76). One sees, that $\Omega_M \approx 0.3$ and $\Omega_\Lambda \approx 0.7$. (Adapted from [22], Fig. 8)

4.8 Inflation

Inflation, first introduced by Alan Guth in 1980 assumes that the expansion of the universe is driven by a scalar field (sometimes there are more than one scalar fields). Using the Lagrangian of a scalar field:

$$L_\Phi = \frac{1}{2} \partial_\mu \Phi \partial^\mu \Phi - V(\Phi), \quad (4.81)$$

one obtains the energy-momentum tensor:

$$T_{\mu\nu} = \partial_\mu \Phi \partial_\nu \Phi - g_{\mu\nu} \left(\frac{1}{2} \partial_\rho \Phi \partial^\rho \Phi - V(\Phi) \right) \quad (4.82)$$

Thus the density and pressure of such a scalar field are given by:

$$\rho_\Phi = T^0_0 = \frac{1}{2} \dot{\Phi}^2 + \frac{1}{2} R^{-2}(t) (\nabla \Phi)^2 + V(\Phi) \approx \frac{1}{2} \dot{\Phi}^2 + V(\Phi) \quad (4.83)$$

$$p_\Phi = \frac{1}{3} T^i_i = \frac{1}{2} \dot{\Phi}^2 - \frac{1}{6} R^{-2}(t) (\nabla \Phi)^2 - V(\Phi) \approx \frac{1}{2} \dot{\Phi}^2 - V(\Phi), \quad (4.84)$$

where it is assumed that the gradient term of the scalar field vanishes in the approximation. The negligence of the gradient term can be motivated by the homogeneity of the CMB, from which one may conclude, that the scalar field was really calm during inflation. Inserting this density and pressure relations into the Friedmann equation 4.62 and the energy conservation equation 4.65, one obtains:

$$H^2 = \frac{8\pi}{3m_{pl}^2} \left(\frac{1}{2} \dot{\Phi}^2 + V(\Phi) \right) \approx \frac{8\pi}{3m_{pl}^2} V(\Phi) \quad (4.85)$$

$$3H\dot{\Phi} = -V'(\Phi) - \ddot{\Phi} \approx -V'(\Phi) \quad (4.86)$$

where the Planck mass $m_{pl}^2 = G$ was introduced and the scalar field is again assumed to be slow: $1/2\dot{\Phi}^2 \ll V(\Phi)$, $\ddot{\Phi} \ll 3H\dot{\Phi}$.

The inflationary dynamics are now discussed using the most simple inflationary potential $V(\Phi) = m^2\Phi^2/2$, referring to [45]. Using this potential, the equations 4.85 and 4.86 get:

$$H^2 \approx \frac{4\pi m^2 \Phi^2}{3m_{pl}^2}, \quad 3H\dot{\Phi} + m^2\Phi \approx 0. \quad (4.87)$$

Combining the equations, one has the solution:

$$\Phi \approx \Phi_i - \frac{m m_{pl}}{2\sqrt{3}\pi} t \quad (4.88)$$

$$a \approx a_i \exp \left[2\sqrt{\frac{\pi}{3}} \frac{m}{m_{pl}} \left(\Phi_i t - \frac{m m_{pl}}{4\sqrt{3}\pi} t^2 \right) \right]. \quad (4.89)$$

The slow-roll parameter ϵ and η , give constraints to the first and second derivative of the potential with respect to Φ . Inflation takes place only if these derivatives are small:

$$\epsilon := \frac{m_{pl}^2}{16\pi} \left(\frac{V'}{V} \right)^2 = \frac{m_{pl}^2}{4\pi\Phi^2} \ll 1 \quad (4.90)$$

$$|\eta| := \left| \frac{m_{pl}^2}{8\pi} \frac{V''}{V} \right| = \left| \frac{m_{pl}^2}{4\pi\Phi^2} \right| \ll 1 \quad (4.91)$$

From this one can conclude the value of the scalar field, at which inflation should end: $|\Phi_f| \approx m_{pl}^2/\sqrt{4\pi}$. By using eq. 4.88 one can calculate the time of the end of inflation and with 4.89 one obtains the number of e-foldings, the universe expands:

$$N = \ln \frac{a_f}{a_i} \approx 2\pi \left(\frac{\Phi_i}{m_{pl}} \right)^2 - \frac{1}{2} \quad (4.92)$$

4.8.1 A typical inflationary universe

Some of the parameters of inflation can be fixed by using the energy scale of reheating, the stage at which the inflaton(= scalar field) decays into radiation and by considering the flatness and horizon problem. In general the energy scale of reheating is assumed to be of the order of the SUSY energy scale, at which the running coupling constants of the electromagnetic, the weak and the strong interaction become equal. This equality happens at about $10^{15} GeV$, corresponding to a temperature of $T = 1.2 \cdot 10^{28} K$. As temperature is inverse proportional to the scale factor a , reheating should happen at about $a = 2.4 \cdot 10^{-28}$.

An estimation of the number of e-foldings produced by inflation can be made by solving the flatness problem: The universe observed today looks really flat. According to [21] the 'curvature density' must be really small: $\Omega_R < 0.02$. Referring to eq. 4.68 till 4.71 the curvature density should have been much more smaller at time-scales of reheating: $\Omega_R < 1.3 \cdot 10^{-53}$. The theory of inflation explains this fine-tuning of the curvature density by the scalar field, which behaves as vacuum energy and drives the curvature density down. Thus, assuming that the radiation density was the vacuum density of the scalar field before reheating, inflation should last at least 26 orders of magnitude, corresponding to $N = 61$ e-foldings, requiring the curvature- and inflaton density were equal at the beginning of inflation. This number of e-foldings yield according to eq. 4.92 to an initial scalar field value of $\Phi \approx 3m_{pl}$.

[46] requires, that $m \approx 10^{-6} m_{pl}$, yielding to a Hubble rate of about $H = 6 \cdot 10^{-6} m_{pl}$. The corresponding horizon scale $R_H = c/H \approx 1.5 \cdot 10^5 l_p$ has to be stretched up to the full sky to explain the homogeneity of the CMB (horizon problem). From eq. 4.59 one sees, that this scale is today about $10R_{H_0}$, where $R_{H_0} = 4.29 Gpc$ is the Hubble radius today. This requires a stretch of about 59.8 orders of magnitude from the begin of inflation till today.

4.9 The Horizon Scale

As mentioned in section 4.4, the Hubble Radius R_H defines a length, at which two objects have moved away from each other with the speed of light in Newtonian approximation. Accordingly at this scale the two distant objects begin to loose their causal contact. For this reason one says that a physical scale λ_{ph} crosses the horizon at $\lambda_{ph} = R_H = \frac{1}{H}$, where c is defined as $c = 1$. One usually uses the comoving scale $\lambda \cdot a = \lambda_{ph}$, which then crosses the horizon at:

$$\lambda = \frac{1}{Ha} \approx \tau, \quad (4.93)$$

where the last approximation can be seen by inserting the scale factors in conformal time dependence of table 4.1. The approximation holds exact, if the initial time- and scale factor constants correspond to the used expansion law. In the real universe the expansion law changes, because the dominating matter types with a different equation of state (ω) change its fraction. Figure 4.3 shows the deviation of the approximation $Ha = \tau^{-1}$.

The horizon crossing condition can be rewritten by the corresponding momentum scale $k \approx \lambda^{-1}$. Horizon crossing happens then at $x := k\tau = 1$. In summary one can distinguish between sub- and super- horizon scales:

Sub horizon scale in causal contact	Super horizon scale not in causal contact
$\lambda < \frac{1}{Ha} \approx \tau$	$\lambda > \frac{1}{Ha} \approx \tau$
$k\tau = x > 1$	$k\tau = x < 1$

Table 4.2: Sub- and Super- horizon scales

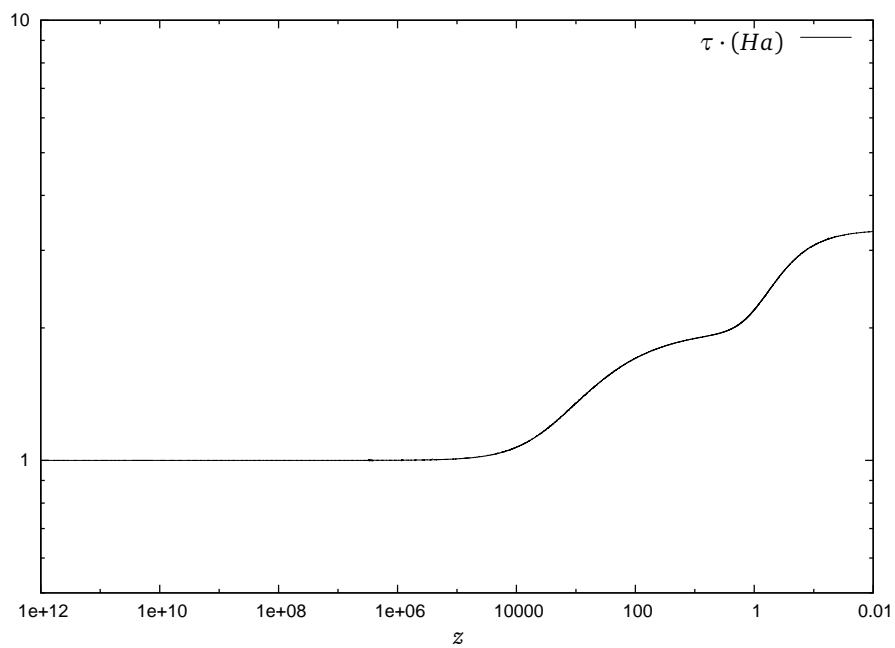


Figure 4.3: $Ha \approx \tau^{-1}$ approximation

$Ha\tau$ is plotted over the redshift z , taken from a cmbeasy run. The approximation is exact as long as the plotted line equals one. When matter begins to dominate, the exactness breaks down. It further deviates during the stage of vacuum domination. The scale $\lambda = \tau$ exceeds the horizon three times then.

5 Cosmological Perturbation Theory

Attention!

The dot denotes no longer a deviation with respect to the physical time $\dot{a} = \frac{da}{dt}$, but a deviation with respect to the conformal time:

$$!!! \quad \dot{a} = \frac{da}{d\tau} \quad !!! \quad \text{From now on.} \quad (5.1)$$

The physics, described in this chapter are be closely related to [4], [25] and [26], because `cmbeasy` is used for the investigation of the perturbation evolution. In the most times, the space-like curvature will be neglected.

5.1 Perturbations of the background quantities

5.1.1 Metric perturbations

The unperturbed metric $\bar{g}_{\mu\nu}$ of eq. 4.37 can be perturbed by adding a small deviation $a^2 h_{\mu\nu}$. Usually the general ansatz for the perturbed metric is:

$$h_{\mu\nu} dx^\mu dx^\nu = -2Ad\tau^2 - 2V_i d\tau dx^i + 2H_{ij} dx^i dx^j \quad (5.2)$$

$$g_{\mu\nu} = \bar{g}_{\mu\nu} + a^2 h_{\mu\nu}, \quad (5.3)$$

where A is a scalar field, $V_i = \phi_{,i} + B_i$ is a vector field, decomposed into a gradient of a scalar $\phi_{,i}$ and a transverse, rotational vector field $B_i, B_i^{,i} = 0$. The tensor field

$$H_{ij} = H_L \gamma_{ij} + \left(\nabla_i \nabla_j - \frac{1}{3} \gamma_{ij} \Delta \right) H_T + \frac{1}{2} \left(H_{ij}^{(V)} + H_{ji}^{(V)} \right) + H_{ij}^{(T)} \quad (5.4)$$

can be decomposed into a trace generating scalar H_L , a 'double gradient' scalar H_T , a transverse vector $H_i^{(V)}, H_i^{(V)i} = 0$ and a transverse traceless tensor $H_{ij}^{(T)}, H_{ij}^{(T)j} = 0, H_i^{(T)i} = 0$. The scalars contribute to one degree of freedom, the vectors to $3 - 1$ constraint = 2 degrees of freedom and the tensor to $6 - (3 + 1)$ constraints = 2, yielding a total number of $1 \cdot 4$ scalar + $2 \cdot 2$ vector + $2 \cdot 1$ tensor = 10 degrees of freedom. This corresponds to $\frac{n(n+1)}{2} = 10$ independent parameters in the 4-metric of the physical space-time.

A harmonic decomposition can be made by using the laplacian eigenfunctions:

$$\Delta Y = -k^2 Y, \quad \Delta Y_j^{(V)} = -k^2 Y_j^{(V)}, \quad \Delta Y_{ji}^{(T)} = -k^2 Y_{ji}^{(T)} \quad (5.5)$$

for each eigenvalue / wave vector k , and defining:

$$Y_j := -k^{-1} Y_{|j}, \quad Y_{ij} := -k^{-2} Y_{|ij} + \frac{1}{3} \gamma_{ij} Y, \quad Y_{ij}^{(V)} := -\frac{1}{2k} \left(Y_{ij}^{(V)} + Y_{ji}^{(V)} \right). \quad (5.6)$$

With this, the decomposition is of the form:

$$A = AY \quad (5.7)$$

$$V_i = BY_i + B^{(V)} Y_i^{(V)} \quad (5.8)$$

$$H_{ij} = H_L Y \gamma_{ij} + H_T Y_{ij} + H^{(V)} Y_{ij}^{(V)} + H^{(T)} Y_{ij}^{(T)} \quad (5.9)$$

Altogether the scalar perturbed metric reads:

$$g_{\mu\nu} = a^2 \begin{pmatrix} -1 - 2AY & -BY_i \\ -BY_j & (1 + 2H_L Y) \gamma_{ij} - 2H_T Y_{ij} \end{pmatrix} \quad (5.10)$$

With this metric, the velocity perturbation in the rest frame results by the normalization condition $g_{\mu\nu}u^\mu u^\nu = -1$ to:

$$u^\mu = \frac{1}{a} (1 - AY, vY^i) \quad , \quad u_\mu = a (1 - AY, (v - B)Y^i) \quad (5.11)$$

The choice of coordinates in general relativity is free. Thus the physics should be independent of a displacement by a small vector $X = T\partial_0 + L^i\partial_i$. This yields the gauge transformation:

$$\tilde{h} = h + a^{-2}L_X \tilde{g} \quad , \quad (5.12)$$

where L_X is the Lie derivative and h is the scalar + vector + tensor perturbation of the metric.

Comparing \tilde{h} and h , one can read off the behavior of the scalar, vector and tensor amplitudes under the gauge transformation:

$$\tilde{A} = A + \frac{\dot{a}}{a}T + \dot{T} \quad (5.13)$$

$$\tilde{B} = B - \dot{L} - kT \quad (5.14)$$

$$\tilde{B}^{(V)} = B^{(V)} - \dot{L}^{(V)} \quad (5.15)$$

$$\tilde{H}_L = H_L + \frac{\dot{a}}{a}T + \frac{k}{3}L \quad (5.16)$$

$$\tilde{H}_T = H_T - kL \quad (5.17)$$

$$\tilde{H}^{(V)} = H^{(V)} - kL^{(V)} \quad (5.18)$$

$$\tilde{H}^{(T)} = H^{(T)} \quad (5.19)$$

It turns out, that the vector perturbations $B^{(V)}$ and $H^{(V)}$ are damped (see [27] and [28]). So they can be neglected today. The obviously gauge invariant metric perturbation $H^{(T)}$ will characterize gravitational waves. Though it is not coupled to the rest of the perturbation variables it will not be treated in the following.

Common known gauges are:

Longitudinal gauge: This gauge is defined by $H_T^{(long)} = 0$ and $B^{(long)} = 0$. The remaining perturbation variables $A = \Psi$ and $H_L = \Phi$ are like the background quantities diagonal entries of the metric and have the meaning of a gravitational potential and a constant curvature. For this reason it is also named **Conformal Newtonian gauge**.

Synchronous gauge: The synchronous gauge is defined by: $A_s = 0$, $B_s = 0$.

One introduces the gauge invariant Bardeen potentials, which are defined as:

$$\Psi = A - \frac{\dot{a}}{a}k^{-1}\sigma - k^{-1}\dot{\sigma} \quad (5.20)$$

$$\Phi = H_L + \frac{1}{3}H_T - \frac{\dot{a}}{a}k^{-1}\sigma \quad , \quad (5.21)$$

$$\text{with } \sigma = k^{-1}\dot{H}_T - B \quad . \quad (5.22)$$

5.1.2 Perturbations of the energy momentum tensor

In the rest frame the general form of the energy momentum tensor

$$T_{\nu}^{\mu} = (\rho + p)u^\mu u_\nu + pg_{\nu}^{\mu} \quad , \quad (5.23)$$

can be rewritten to an eigenvector problem by multiplying u^ν :

$$T_{\nu}^{\mu}u^\nu = -\rho u^\mu \quad (5.24)$$

Requiring a density and pressure perturbation:

$$\rho = \bar{\rho}(1 + \delta Y) \quad , \quad p = \bar{p}(1 + \pi_L Y) \quad , \quad (5.25)$$

and an anisotropic, traceless ($\Pi_j^{i(full)} = 0$), space-like pressure perturbation (named **shear**):

$$\Pi_j^{i(full)} = \Pi Y_j^i + \Pi^{(V)}Y_j^{(V)i} + \Pi^{(T)}Y_j^{(T)i} \quad (5.26)$$

one ends up with the perturbed energy momentum tensor

$$T_\nu^\mu = \begin{pmatrix} -\bar{\rho}(1 + \delta Y) & -\bar{\rho}(1 + \omega)vY^i \\ \bar{\rho}(1 + \omega)(v - B)Y_j & \bar{p}\delta^i_j(1 + \pi_L Y) + \bar{p}\Pi Y_j^i \end{pmatrix} \quad (5.27)$$

where the vector and tensor part of the shear are neglected.

One can now construct common used gauge invariant density and velocity perturbations:

$$D_g = \delta + 3(1 + \omega) \left(H_L + \frac{1}{3} H_T \right) = \delta^{(long)} + 3(1 + \omega)\Phi \quad (5.28)$$

$$D = \delta^{(long)} + 3(1 + \omega)\mathcal{H} \frac{V}{k} \quad (5.29)$$

$$V = v^{(long)} = v - \frac{1}{k} \dot{H}_T \quad (5.30)$$

$$\Gamma = \pi_L - \frac{c_s^2}{\omega} \delta \quad (5.31)$$

$$(5.32)$$

Evolution equations for density perturbations

Finally one may derive the perturbed Einstein equations:

$$4\pi G a^2 \rho D = k^2 \Phi \quad (00) \quad (5.33)$$

$$4\pi G a^2 (\rho + p) V = k (\mathcal{H} \Psi - \dot{\Phi}) \quad (0i) \quad (5.34)$$

$$-k^2 (\Phi + \Psi) = 8\pi G a^2 p \Pi \quad (5.35)$$

and the conservation equations (applying $T^{\mu\nu}_{;\nu}$):

$$\dot{D}_g + 3(c_s^2 - \omega)\mathcal{H} D_g + (1 + \omega)kV + 3\omega\mathcal{H}\Gamma = 0 \quad (00) \quad (5.36)$$

$$\dot{V} + \mathcal{H}(1 - 3c_s^2)V = k(\Psi - 3c_s^2\Phi) + \frac{c_s^2 k}{1 + \omega} D_g + \frac{\omega k}{1 + \omega} \left(\Gamma - \frac{2}{3} \Pi \right) \quad (0i) \quad (5.37)$$

These are only the equations for the scalar density perturbations. The equations for vector and tensor perturbations can be found in [4]. An elaborate derivation of the equations is given in [27].

In the fluid- and scalar-field case the equations 5.33 till 5.37 can be reduced to:

$$\ddot{\Psi} + 3\mathcal{H}(1 + c_s^2)\dot{\Psi} + [(1 + 3c_s^2)\mathcal{H}^2 - (1 + 3\omega)\mathcal{H}^2 + \Upsilon k^2]\Psi = 0, \quad (5.38)$$

where $\Upsilon = c_s^2$ for a fluid and $\Upsilon = 1$ for a scalar field.

This equation can be reformulated by using the variables:

$$u = a \left[4\pi G (\mathcal{H}^2 - \dot{\mathcal{H}}) \right]^{-\frac{1}{2}} \Psi, \quad \theta = \frac{3\mathcal{H}}{2a\sqrt{\mathcal{H}^2 - \dot{\mathcal{H}}}}, \quad (5.39)$$

yielding to:

$$\ddot{u} + \left(\Upsilon k^2 - \frac{\ddot{\theta}}{\theta} \right) u = 0. \quad (5.40)$$

cmbeasy uses the equations 5.36 and 5.37 together with the equations 5.33 and 5.35 to evolve the perturbation variables along conformal time. For that the equations are extended to a multi-component system and the equation of state (ω) is inserted. Baryons and CDM have no pressure $\Rightarrow \omega_b = \omega_m = 0$ and photons and relativistic neutrinos have $\omega_\gamma = \omega_\nu = \frac{1}{3}$. In the multi-component system an energy momentum transfer $\tilde{T}_{(\alpha)\mu;\nu}^v = \tilde{Q}_{(\alpha)\mu}$ is possible, but the sum of the energy momentum transfers $\sum_\alpha \tilde{Q}_{(\alpha)\mu} = 0$ must vanish due to energy momentum conservation. The index (α) denotes the different species of matter: $\alpha \in \{c, b, \gamma, \nu\}$. In Friedmann cosmology the different species are treated separately from each other. Therefore the question arises if there is a non-vanishing energy momentum transfer.

Using [29], Compton scattering which couples baryons and photons is taken into account.

5.2 Initial Conditions

According to [25] the equations 5.36 and 5.37 are simplified corresponding to the stage of the universe far before recombination and re-parameterized to equations, that depend on $x = k\tau$, instead of τ . The differential equation can be written in matrix notation $\frac{d}{d \ln x} U = AU$, were A is a matrix and $U = (D_{gc}, x^{-1}V_c, D_{g\gamma}, x^{-1}V_\gamma, D_{gb}, x^{-1}V_b, D_{gv}, x^{-1}V_v, x^{-2}\Pi_v)$ is the vector of perturbation variables. Further considerations yield, that the first order approximation $U(x) = \sum_i c_i \left(\frac{x}{x_0}\right)_i^\lambda U_i$ has four non-decaying modes U_i which remain constant ($\lambda_i = 0$).

A further distinction of the modes can be made by using the multi-component entropy perturbation $\Gamma = \Gamma_{int} + \Gamma_{rel}$. The internal entropy perturbations $\Gamma_{int} = \sum_\alpha \Gamma_\alpha$ of the matter species (α) are obviously assumed to vanish in the common literature. Assuming that the energy momentum transfer $Q_{(\alpha)\mu}$ of the matter species can be neglected the relative entropy perturbation can be written as ([27], [3]):

$$\Gamma_{rel} = \frac{1}{2p} \sum_{\alpha, \beta} \frac{(\rho_\alpha + p_\alpha) \cdot (\rho_\beta + p_\beta)}{\rho + p} (c_\alpha^2 - c_\beta^2) S_{\alpha\beta} \quad (5.41)$$

$$\text{with } S_{\alpha\beta} = \frac{D_\alpha}{1 + \omega_\alpha} - \frac{D_\beta}{1 + \omega_\beta} \quad (5.42)$$

, were α and β are matter species indices. From this one concludes, that two matter species are adiabatic, if $S_{\alpha\beta} = 0$ is satisfied. As a result the density perturbations have the specific fraction $3D_v = 3D_\gamma = 4D_c = 4D_b$ if they are adiabatic.

6 The cmbeasy program

The integration of the perturbation equations (5.33 - 5.37) is done with `cmbeasy` (www.cmbeasy.de). `cmbeasy` is a C++ code, which calculates the spherical harmonic decomposition of the temperature-temperature power spectrum of the CMBR anisotropy. It originates from the Fortran code `cmbfast`. `cmbeasy` is also used for handle quintessence models, which are candidates for describing dark energy.

6.1 Short description

The compilation is managed by `cmake`. The command line version of `cmbeasy` is executed by the `xcmb` command, which calls the `xdriver.main()` function and accesses its configuration from the `configuration.cfg` file. There is also a graphical user interface (GUI) available by executing `cmbeasy`, which creates an instance of `CmbMainWindow`. Though the GUI is more suggestive, the command line version will be regarded, because it is easier to trace back the exact program flow.

The (for this work) most important stages of the program are shown in figure 6.1. In principle the program first integrates the Friedmann equation 4.62, to get the homogeneous densities of the different matter species and the Hubble constant at every time. With this, the equations 5.33 - 5.37 can be solved by integration, where some initial conditions have to be set up first. Although there are also iso-curvature initial conditions, this work will only consider adiabatic initial conditions. Then the harmonical decomposition of the density perturbations at the stage of recombination is obtained by using the perturbed Boltzmann equation rewritten along geodesics. The result is the temperature anisotropy power spectrum.

Note that a lot of simplifications have been made in figure 6.1. Some of them are:

1. `cmbeasy` calls the instances of `DataManager`, `ControlPanel`, `Cosmos`, `CmbCalc`, `Perturbation`, `AnalyzeThis`, not the raw classes itself.
2. All if clauses (some preventing functions to be called) are not shown.

6.2 Configuration and Properties

Background parameters of the universe are taken from [21]:

$$\Omega_\Lambda = 72.1\% \quad , \quad \Omega_c = 23.3\% \quad , \quad \Omega_b = 4.6\% \quad , \quad \Omega_K = 0 \quad , \quad H_0 = 70.1 \frac{km}{s \text{ Mpc}} \quad , \quad n_s = 0.96 \quad (6.1)$$

The curvature density is assumed to be zero, because there is no current evidence for curvature and it is not implemented in `cmbeasy`.

There are several derivatives of the `Cosmos` and `Perturbation` class, namely `QuintCosmos` and `SpeedyInvariant`, `SpeedyDEInvariant`, `Synchronous` and `QuintSynchronous`. `Quint` and `DE` stands for Dark Energy or Quintessence, `Invariant` for gauge invariant and `Synchronous` for the synchronous gauge.

`cmbeasy` is used with the default settings which are `QuintCosmos` for the `Cosmos` class and `SpeedyInvariant` for the `Perturbation` class. The quintessence density Ω_q is set to zero in `QuintCosmos`, to get a quintessence-free behavior of the cosmos.

6.3 The Evolution of Perturbations

Using the program configuration described above with adiabatic initial conditions, one can investigate the evolution of the perturbation variables. This is done in figure 6.2 by writing out the variables during the integration process along conformal time. `cmbeasy` performs this integration on a series of different k -modes, shown in figure 6.3 and 6.4. The initial powerlaw spectrum gets modified by the growth of the perturbation variables, which is in principle imprinted in the

CDM density perturbation today. Unfortunately the oscillation frequency increases for higher k -modes, requiring more time-steps (see figure 6.6). More problematical is a strong growth of the perturbation variables at high k , shown in figure 6.5. Although the unusual behavior of V_γ begins at about $k = 20h \cdot Mpc^{-1}$, D_{gc} grows only at higher k ($k = 110 \cdot hMpc^{-1}$). The reason is that V_γ has first to grow on the order of magnitude of D_{gc} , before D_{gc} is affected by V_γ .

cmbeasy work flow

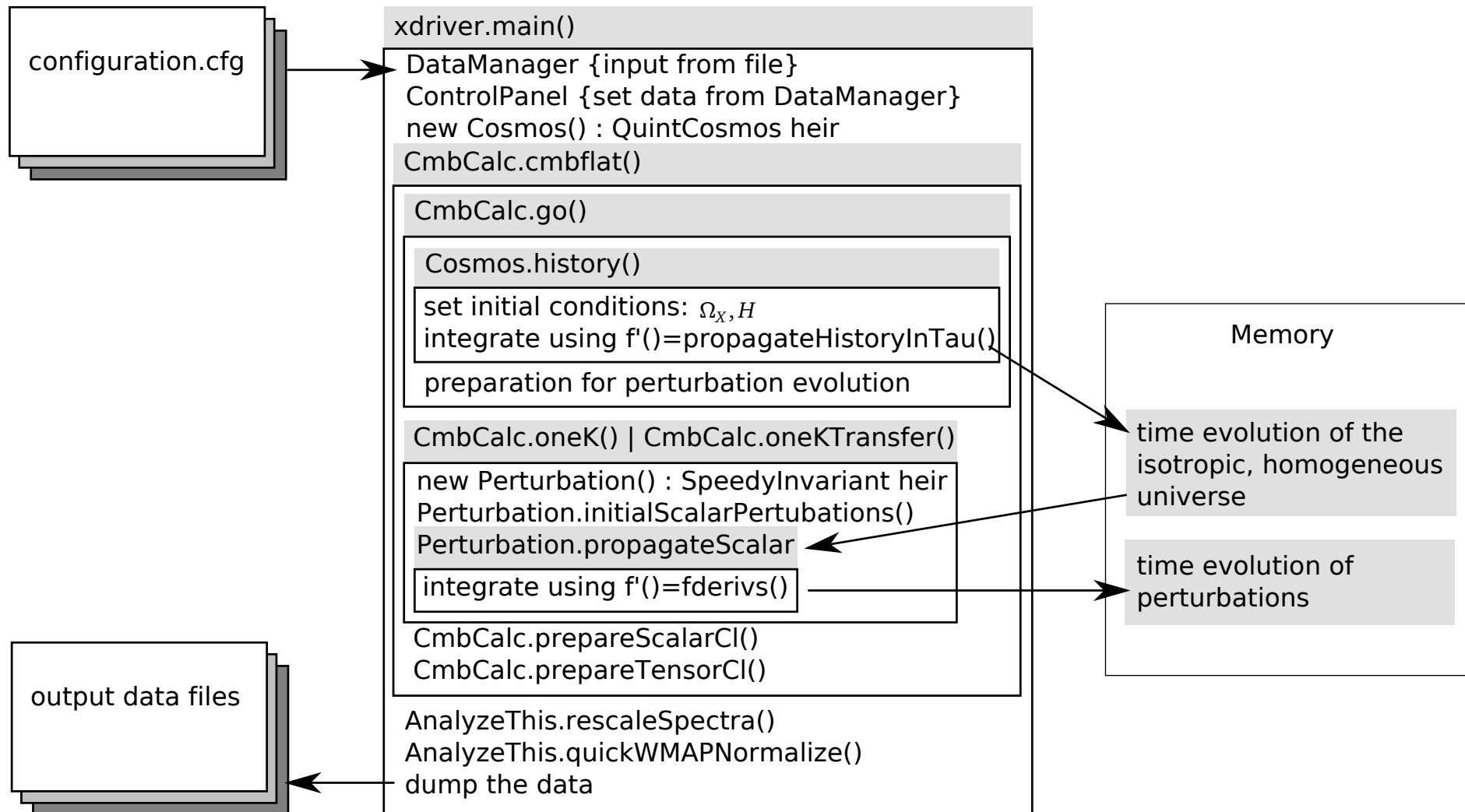


Figure 6.1: A sketch of a `cmbeasy` run. First `DataManager` reads out `configuration.cfg` and sets up `ControlPanel`. Then the background quantities of the homogeneous and isotropic universe of the Friedmann equation 4.77 are calculated with `Cosmos`. This background is used for a second integration of the perturbation equations along conformal time τ by `Perturbation`. At the end the CI's are calculated. `CmbCalc` has the meaning of a calculation administration.

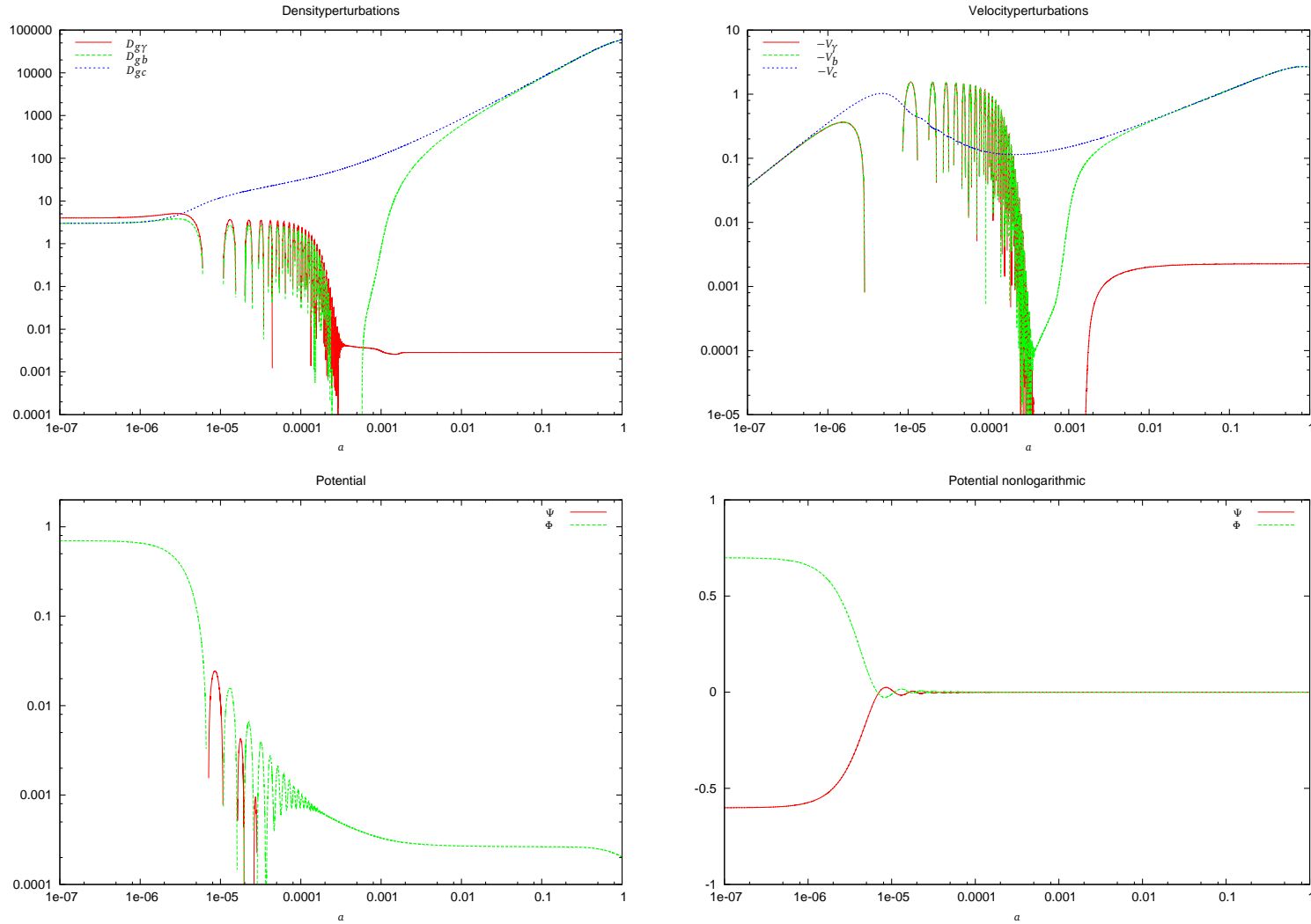


Figure 6.2: Evolution of the Density, Velocity and Potential Perturbations

The perturbation has a momentum scale of $k = 3.7h Mpc^{-1}$, corresponding to an extension of $\lambda = 1.7h^{-1} Mpc$. Scale factor a is used as association of time. Neutrino perturbation is not shown in the plots, because it would contribute only during radiation dominance, where it oscillates with the photon perturbation. Shear is negligible too because of relation (5.35) and the lower right plot.

The perturbation evolution behaves as described in the literature: At the beginning density and potential variables remain constant until they enter the horizon, which happens at $a(x)|_{1,0} = 8.3 \cdot 10^{-7}$. Now radiation pressure forces a start of oscillations of the perturbations. These repulsive forces drive the gravitational potential (Φ and Ψ) down as shown in the lower plots. At $a = 3 \cdot 10^{-4}$ the oscillations are damped by photon diffusion. After recombination at $a = 8.8 \cdot 10^{-4}$ baryons decouple from photons and are dragged into the CDM potential.

Perturbation evolution

Baryon density —

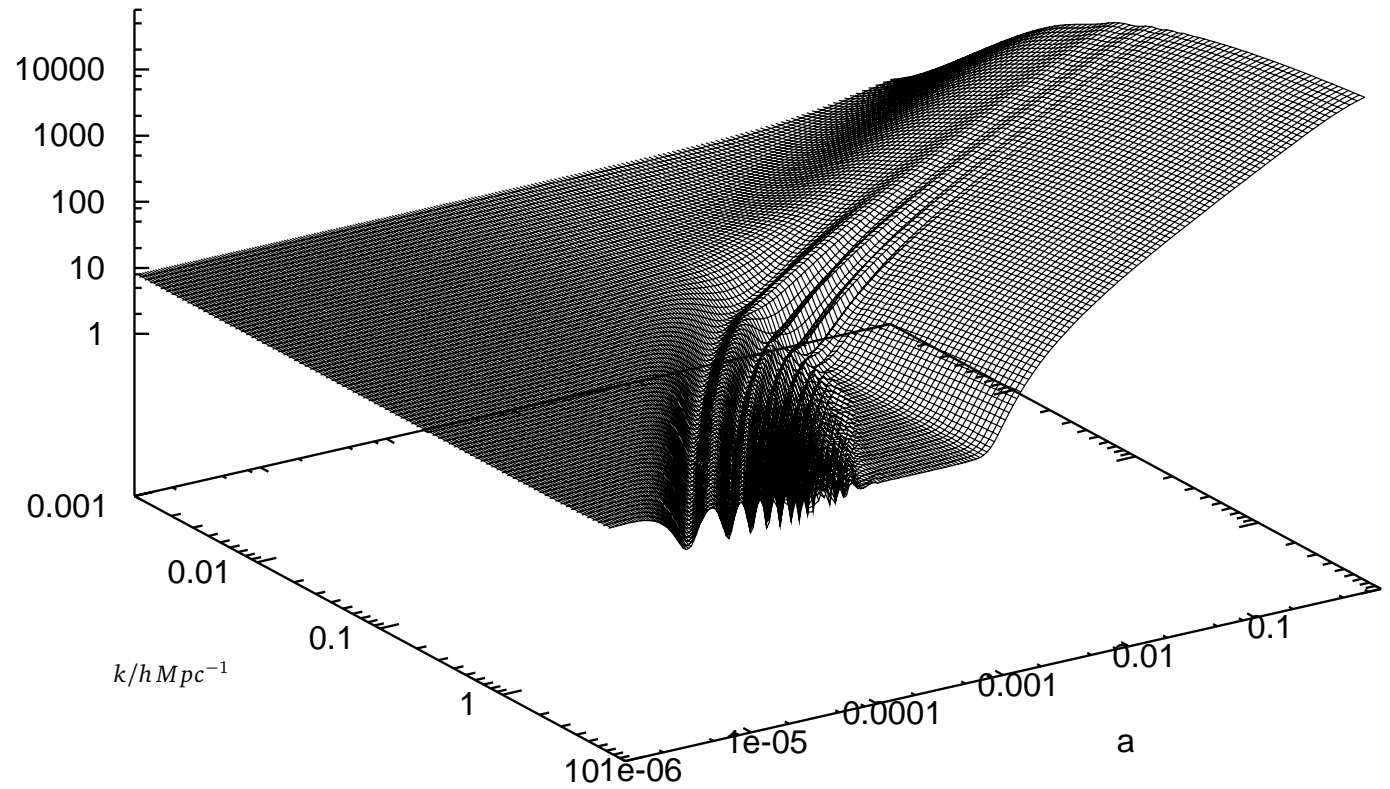


Figure 6.3: The evolution of all baryon density perturbation modes is shown. To resolve the baryonic acoustic oscillations in the logarithmic plot the value of the perturbation variable has been increased by the a small constant 5. The time is growing along the scale factor a and the length scale of the mode is given by it's wavenumber k .

Perturbation evolution

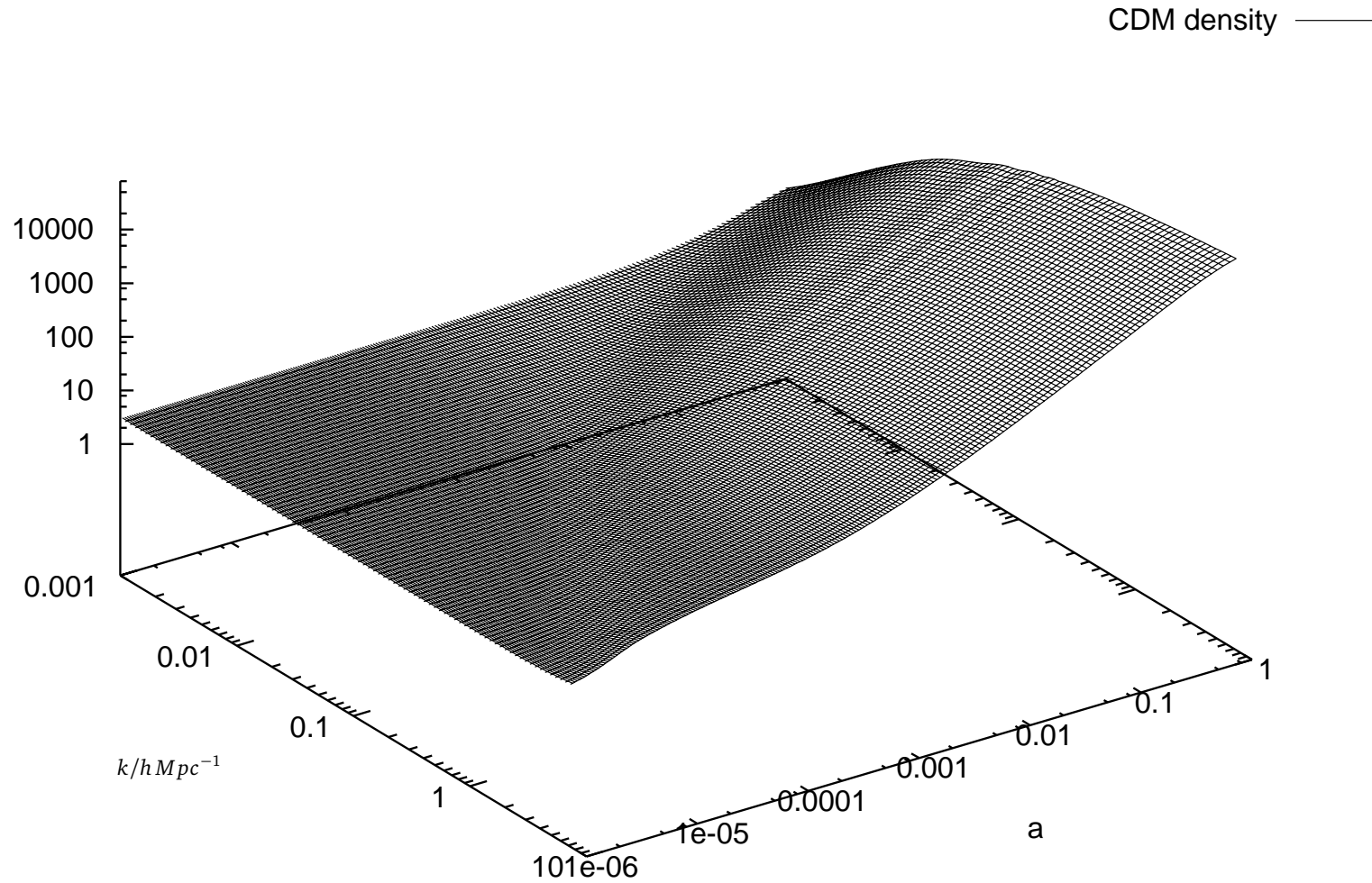


Figure 6.4: The evolution of all CDM density perturbation modes is shown. The axes are the same as in fig. 6.3. The oscillations, which are present at recombination (neither super horizon nor damped away) cause an imprint in the CDM and thus occur in the power spectrum of the matter density distribution of the universe.

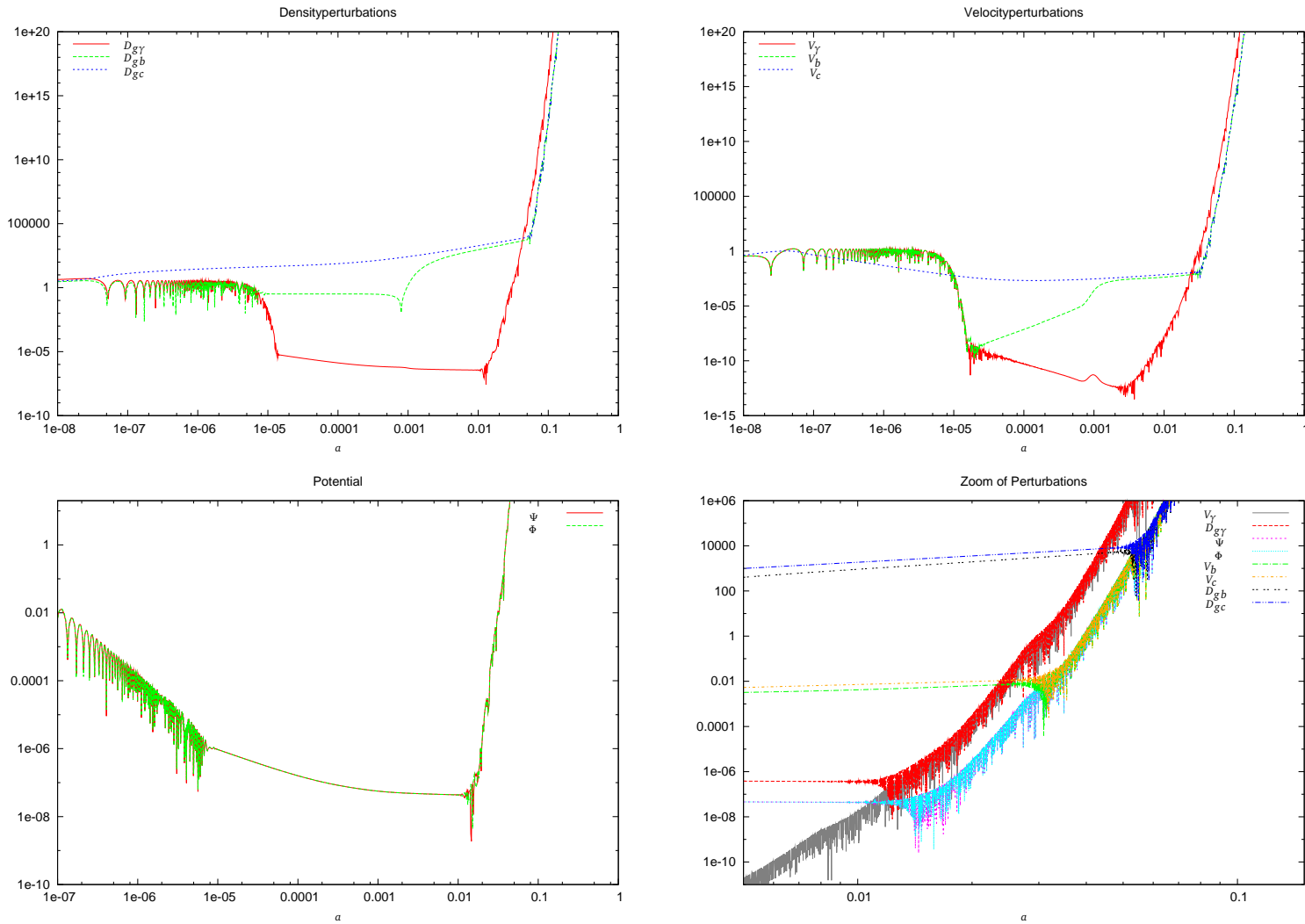


Figure 6.5: Breakdown of perturbation evolution

The perturbation has a momentum scale of $k = 428.0h Mpc^{-1}$, corresponding to an extension of $\lambda = 14.7h^{-1}kpc$. The plots are of the same type as in figure 6.2 except the zoom-plot in the lower-right. Note that the absolute value of the perturbation variables is plotted because they change their signs (even CDM), yielding to a frayed plot.

Obviously the photon velocity V_γ grows, which causes a successive drag of the other variables: First $D_{g\gamma}$, then Ψ & Φ , V_b , V_c , D_{gb} and D_{gc} grow nearly unlimited. It is rather unphysical that V_γ is growing after recombination. Maybe the weak coupling approximation of baryons and photons breaks down at high k .

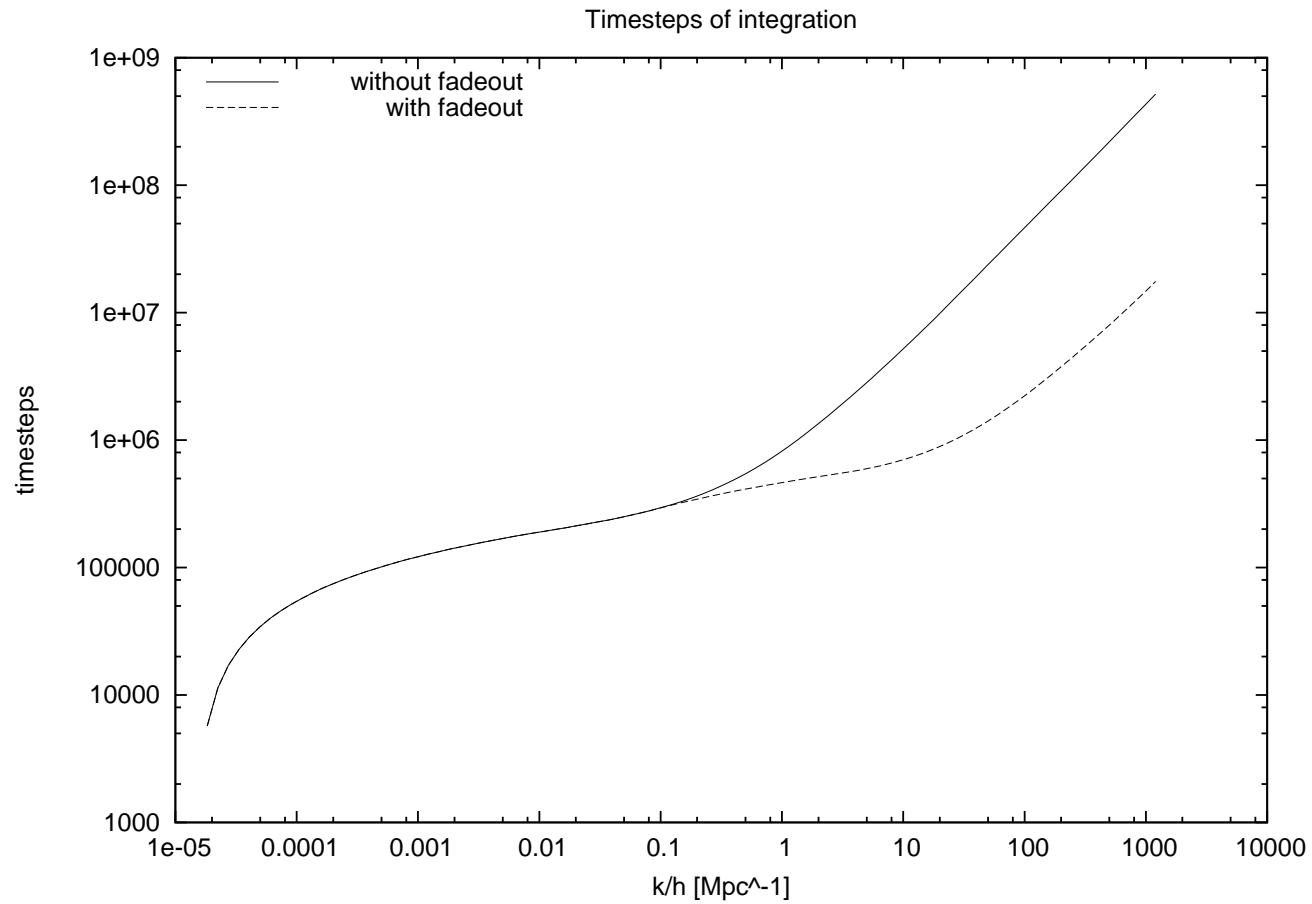


Figure 6.6: The number of time-steps required for one run of cmbeasy is plotted over the corresponding mode k . To improve the integration speed and reduce the number of time-steps a fadeout is introduced in cmbeasy. The fadeout damps oscillations at 'late times'. This damping may influence the perturbation evolution on small scales and is disabled in this work for this reason.

7 Power Spectra

7.1 Conventions

It is known, that Inflation has produced a nearly scale invariant power spectrum, given as primordial curvature perturbation:

$$\Delta_{\text{R}}^2(k) = \frac{k^3 P_{\text{R}}(k)}{2\pi^2} = \Delta_{\text{R}}^2(k_0) \left(\frac{k}{k_0} \right)^{n_s(k_0) - 1 + \frac{1}{2} \frac{dn_s}{d \ln k}}, \quad (7.1)$$

, where $\Delta_{\text{R}}^2(k_0)$ is a specific amplitude of the power spectrum at a given scale k_0 . The connection between power spectrum and momentum space amplitude R_k is given via the fluctuation $\langle \Delta^2 \rangle$:

$$\langle \Delta^2 \rangle := \frac{V}{(2\pi)^3} \int d^3k |R_{pl}|^2 = \frac{V}{2\pi^2} \int k^2 dk |R_{pl}|^2 = \frac{V}{2\pi^2} \int k^2 dk P_{\text{R}}(k) = \frac{V}{2\pi^2} \int k^3 d \ln k P_{\text{R}}(k) = V \int d \ln k \Delta_{\text{R}}^2(k), \quad (7.2)$$

which explains the factor k^3 .

Here the curvature perturbation can be introduced:

$$R_{pl} = (P_{\text{R}}(k))^{\frac{1}{2}} \quad (7.3)$$

and relate it to the density according to the approach in [30] and [3]:

$$\left(\frac{aH}{k} \right)^2 D_{pl} = \frac{2(1+\omega)}{5+3\omega} R_{pl}, \quad (7.4)$$

where the index pl stands for the powerlaw version of the variable: $R_{pl} = R/k^{\frac{3}{2}}$.

The consideration of curvature perturbation suggests, that longitudinal gauge (just isotropic perturbations) has to be applied. Therefore it stands to reason to use the gauge invariant density perturbation D , as in [3].

Using the Poisson equation (5.33) one may relate D to Φ :

$$\Phi_{pl} = \left(\frac{aH}{k} \right)^2 \frac{3}{2} D_{pl} = \frac{3(1+\omega)}{5+3\omega} R_{pl} = K_{\Phi\text{R}} R_{pl}, \quad K_{\Phi\text{R}} := \frac{3(1+\omega)}{5+3\omega} = \frac{2}{3}, \quad (7.5)$$

where radiation domination during the initial phase of the universe is assumed for $K_{\Phi\text{R}}$.

The power spectrum of the density, potential and curvature perturbation can also be related to the temperature anisotropy of the CMB during recombination. Therefore equations 5.36, 5.37 and 5.33 can be solved analytically to obtain some initial conditions. According to the approach in [4] one gets on super horizon scales for adiabatic initial conditions the approximation:

$$\frac{4}{3} D_{gmpl} = D_{grpl} \approx -\frac{20}{3} \Psi_{pl}, \quad V_{rpl} = V_{mpl} \approx \frac{1}{3} x \Psi_{pl}, \quad \Psi_{pl} = \Psi_{0pl} = \text{const.}, \quad (7.6)$$

where $\Phi_{pl} = -\Psi_{pl}$ is assumed (see fig. 6.2).

Referring again to [4] the direction (n) dependent temperature difference of CMB measured today is given by:

$$\frac{\Delta T(n)}{T} = \left[\frac{1}{4} D_{grpl} + V_{bjpl} n^j + \Psi_{pl} - \Phi_{pl} \right] (\eta_{dec}) + \int_{\eta_{dec}}^{\eta_0} (\dot{\Psi}_{pl} - \dot{\Phi}_{pl}) d\eta \quad (7.7)$$

and inserting 7.6 by neglecting small V and ISW $\dot{\Psi} - \dot{\Phi}$ one obtains:

$$\left(\frac{\Delta T(n)}{T} \right)^{(\text{OSW})} \approx \frac{1}{3} \Psi_{pl}(\eta_{dec}, x_{dec}) = \sum_{lm} a_{lm} Y_{lm}. \quad (7.8)$$

The right hand side of equation 7.8 is a decomposition into spherical harmonics Y_{lm} . Correlating the temperature by using $\langle a_{lm} a_{l'm'}^* \rangle = C_l \delta_{ll'} \delta_{mm'}$ (see [4] eq. 4.20 for explanation) yields to:

$$\left\langle \frac{\Delta T(n)}{T} \frac{\Delta T(n')}{T} \right\rangle = \sum_{l,m,l',m'} \langle a_{lm} a_{l'm'}^* \rangle Y_{lm}(n) Y_{l'm'}(n') = \sum_l C_l \frac{2l+1}{4\pi} P_l(n \cdot n') \quad (7.9)$$

Performing on the other hand a Fourier transform by using a decomposition containing spherical Bessel functions j_l one ends up with:

$$\left\langle \frac{\Delta T(n)}{T} \frac{\Delta T(n')}{T} \right\rangle = \sum_l \frac{2}{\pi} \int \frac{dk}{k} k^3 \left\langle \left| \frac{\Psi_{pl}}{3} \right|^2 \right\rangle j_l^2 \frac{2l+1}{4\pi} P_l(n \cdot n') \quad (7.10)$$

Now refer to [31]. By using the power spectrum:

$$|\Psi_{pl}|^2 \approx |\Phi_{pl}|^2 = |K_{\Phi R} R_{pl}|^2 = K_{\Phi R}^2 P_R(k) = K_{\Phi R}^2 \frac{\Delta_R^2(k_0)}{k^3} \left(\frac{k}{k_0} \right)^{n_s(k_0)-1 + \frac{1}{2} \frac{dn_s}{d \ln k}} = \frac{A_\Phi^2}{k^3} \left(\frac{k}{k_0} \right)^{n_s(k_0)-1} \quad (7.11)$$

and assuming $n_s = 1$ and $dn_s/d \ln k = 0$ one may identify and further simplify:

$$C_l^{(SW)} = \frac{2}{\pi} \int \frac{dk}{k} k^3 \left\langle \left| \frac{\Psi_{pl}}{3} \right|^2 \right\rangle j_l^2 = \frac{A_\Phi^2}{9} \left(\frac{1}{k_0 d_A} \right)^{n_s-1} \frac{2^{n_s-3} \Gamma(3-n_s) \Gamma((2l+n_s-1)/2)}{\Gamma^2((4-n_s)/2) \Gamma((2l+5-n_s)/2)} = \quad (7.12)$$

$$= \left(\frac{A_\Phi}{3} \right)^2 \frac{2^{-2} \Gamma(2) \Gamma(l)}{\Gamma^2(3/2) \Gamma(l+2)} = \left(\frac{A_\Phi}{3} \right)^2 \frac{1}{\pi \cdot l(l+1)}. \quad (7.13)$$

One may now read off the amplitude of the power spectrum A_Φ by considering the fluctuations per decade of the super horizon scale in the CMB:

$$\left\langle \frac{\Delta T}{T} \frac{\Delta T}{T} \right\rangle = \sum_l C_l \frac{2l+1}{4\pi} \approx \int \frac{l(l+1) C_l}{2\pi} d \ln l, \quad \frac{l(l+1) C_l^{(SW)}}{2\pi} = \left(\frac{A_\Phi}{3} \right)^2 \frac{1}{2\pi^2} \quad (7.14)$$

7.2 Comparison with measurements

The largest scales of the CMB are located at small l in the angular power spectrum of the temperature anisotropy, namely the Sachs Wolfe plateau in the area of $l \in [2, \dots, 100]$. A fit in the range $l \in [10, \dots, 30]$ yields to the amplitude $l(l+1)C_l/(2\pi) = 862.6 \mu K^2/T^2$ with $T = 2.725K$. As a result one obtains $A_\Phi = 1.437 \cdot 10^{-4}$ sometimes the factor $2\pi^2$ on the right hand side of equation 7.14 is neglected, resulting to an amplitude $A'_\Phi = 3.233 \cdot 10^{-5}$.

The approximation $n_s = 1$ of the spectral index was required for deriving equation 7.13 but is not correct in general. According to [21] n_s will be set to 0.96. Therefore the momentum scale of the spectrum normalization is not irrelevant. The amplitude of SW has been taken at about $l = 20$, corresponding to (eq. 4.59):

$$k_0 = \frac{2\pi}{\lambda} = \frac{2\pi}{3.342 \cdot R_H \Delta\theta} = \frac{2\pi l}{3.342 \cdot R_H 2\pi} = \frac{l}{3.342 \cdot R_H} = \frac{l}{14.2 Gpc} = 0.00141 Mpc^{-1} \quad (7.15)$$

The corrections for a running spectral index are not considered here ($dn_s/d \ln k = 0$).

The resulting power spectra are:

$$\Delta_\Phi^2(k) = A_\Phi^2 \left(\frac{k}{k_0} \right)^{n_s-1} = (1.437 \cdot 10^{-4})^2 \left(\frac{k \cdot Mpc}{0.00141} \right)^{0.96-1} \quad (7.16)$$

$$(\Delta'_\Phi(k))^2 = (A'_\Phi)^2 \left(\frac{k}{k_0} \right)^{n_s-1} = (3.233 \cdot 10^{-5})^2 \left(\frac{k \cdot Mpc}{0.00141} \right)^{0.96-1} \quad (7.17)$$

According to eq. 7.11 the relation $\Delta_\Phi^2(k) = K_{\Phi R}^2 \Delta_R^2(k)$ should hold. A serious estimation of the power spectrum is given in [21] by using cmbfast:

$$k_0 = 0.002 Mpc^{-1}, \quad \Delta_R^2(k_0) = 2.457_{-0.093}^{+0.092} \cdot 10^{-9}, \quad n_s = 0.96_{-0.013}^{+0.014} \quad (7.18)$$

From this the fractions $\frac{\Delta_\Phi^2(k)}{K_{\Phi R}^2 \Delta_R^2(k)} = 18.65$ and $\frac{(\Delta'_\Phi(k))^2}{K_{\Phi R}^2 \Delta_R^2(k)} = 0.9439$ are resulting. Obviously $(\Delta'_\Phi(k))^2 K_{\Phi R}^2 \approx K_{\Phi R}^2 \Delta_R^2(k)$ holds and the question comes up, why the factor of $2\pi^2$ on the right hand side of equation 7.14 can be neglected.

cmbeasy produces a CDM power spectrum by using the value of the CDM density perturbation variable today $D_{gc}(a)|_1$, which can be seen as the top right border of the plotted surface in fig. 6.4. By default cmbeasy uses the power normalization:

$$\Delta_{CDM}^2(k) = D_{gc}^2 A_s \left(\frac{k \cdot Mpc}{0.05} \right)^{n_s-1}, \quad A_s = 20 \cdot 10^{-10}, \quad (7.19)$$

where A_s is the initial scalar power amplitude. Using a built-in routine, which fits the calculated angular power spectrum with the binned temperature anisotropy of the CMB measured by the WMAP satellite (the five year release of the WMAP data is used) `cmbeasy` obtains the normalization $A_s = 21.98 \cdot 10^{-10}$. To check whether the normalization amplitudes of the power spectra of `cmbeasy` and `cmbflat` are in line with each other, the density perturbation has to be replaced by the potential:

$$\Delta_\Phi^2(k) = \Phi^2 A_s \left(\frac{k \cdot Mpc}{0.05} \right)^{n_s - 1}, \quad A_s = 21.98 \cdot 10^{-10}. \quad (7.20)$$

Using the potential at super horizon scales $\Phi = 0.6993$, one obtains $\frac{\Delta_\Phi^2(k)}{K_{\Phi_R}^2 \Delta_R^2(k)} = 1.120$ a rather huge deviation. The fraction using the CDM matter power $\frac{\Delta_{CDM}^2(k)}{\Delta_R^2(k)} = 1.0175$ is surprisingly close to that of the curvature perturbation.

7.3 Evolution of the power spectrum

Using the power normalization of `cmbeasy` described in the above section, the evolved power spectrum can be plotted by using eq. 7.19, as it is shown in figure 7.1.

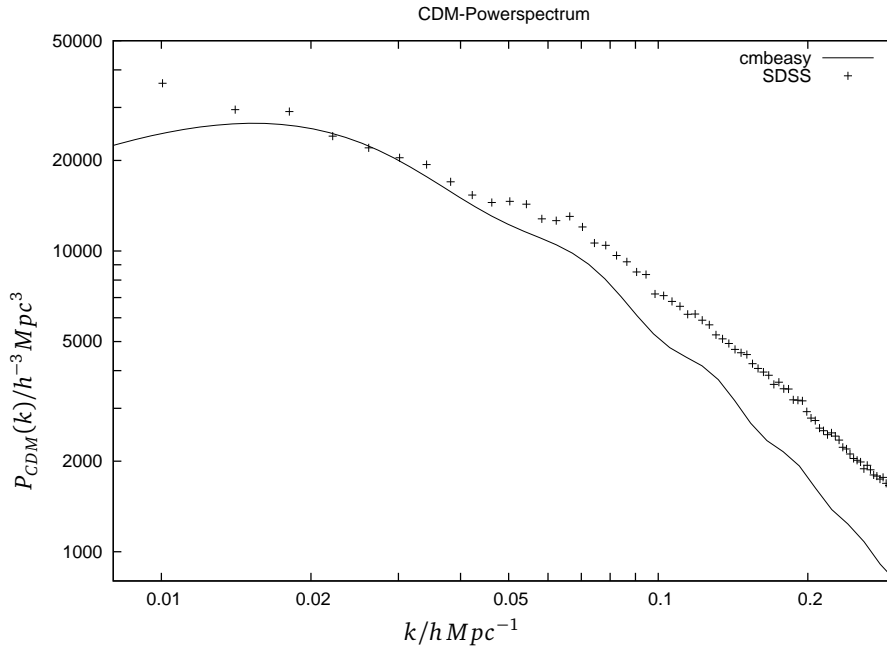


Figure 7.1: The CDM power spectrum $P_{CDM}(k)$ is plotted over the momentum scale k/h . The continuous line shows the evolved CDM spectrum according to eq. 7.19 calculated by `cmbeasy`. The crosses are data from the combined SDSS main galaxy and LRG sample, originally plotted in figure 12 of [32]. The `cmbeasy` spectrum is a bit lower than the spectrum shown in the original figure data but matches in the range of $0.01 < k < 0.03 \cdot h \cdot Mpc^{-1}$. On small scales nonlinear effects become dominant.

7.3.1 The Transferfunction

It is useful to describe the power spectrum by using transfer functions, because there exists an analytic approach, given by Hu and Sugiyama [33], [34], [35], which opens the opportunity to circumvent the integration problems of `cmbeasy` on small scales (see section 6.3). The power spectrum today can be written as:

$$P(k) = A k^{n_s} T^2(k), \quad (7.21)$$

with the transfer function [35]:

$$T(k) \approx \alpha \frac{\ln(1.8\beta q)}{14.2q^2} = 0.89 \frac{\ln(15.9k \cdot Mpc)}{783k^2 \cdot Mpc^2}, \quad q = \frac{k \cdot Mpc \cdot T_0^2}{(\Omega_b + \Omega_c)h^2(2.7K)^2}. \quad (7.22)$$

$\alpha(\Omega_b, \Omega_c) = 0.8873$ and $\beta(\Omega_b, \Omega_c) = 1.1903$ are functions given in eq. E-12 and E-13 of [35] and are calculated with the parameters mentioned in section 6.2.

To be an appropriate continuation of the CDM power spectra of *cmbeasy* the amplitude of the 'analytic' power spectrum has to be fitted to that of *cmbeasy*. A fit in the range $k \in [40 \dots 82] h Mpc^{-1}$ yields to $A = 7.612 \cdot 10^6$. The result can be seen in figure 7.2

7.3.2 Nonlinear growth

The linear perturbed Einstein equations as described in section 5 hold only as long as the density fluctuation $\Delta_{CDM}^2(k)$ is lower than one. Since $\Delta_{CDM}^2(k)$ is in principle the fraction of the fluctuation maximum over the average, linear perturbation theory breaks down and nonlinear effects have to be taken into account when $\Delta_{CDM}^2(k)$ reaches unity.

The nonlinear evolution was already treated by [37], [38] and [39] by giving a fitting function. The ansatz they made was a function f_{NL} , which only depends on the amplitude of the density fluctuations and returns the higher amplitude of the nonlinear density fluctuations: $\Delta_{NL} = f_{NL}(\Delta_L)$. Unfortunately the parameter set of the fitting functions is usually determined for a power spectrum $P(k) = Ak^n$, with $n \in [-2 \dots 0]$. In this work an approximation for high k , requiring $n \approx -3$ would be desirable. Therefore the unfitted data of the Millennium simulation will be used. The millennium simulation is a N-body simulation using $N = 10^{10}$ particles with the initial cosmological parameters:

$$\Omega_b = 0.045 \quad , \quad \Omega_c = 0.205 \quad , \quad \Omega_\Lambda = 0.75 \quad , \quad H_0 = 73 \frac{km}{s \cdot Mpc} \quad , \quad n_s = 1 \quad . \quad (7.23)$$

The chosen parameters are close to those used in this work and correspond to a power spectrum $P(k) \approx Ak^{-3}$, as needed. The Millennium simulation is therefore a good nonlinear continuation of the perturbation evolution of *cmbeasy* in the concordance model. Nevertheless, the underlying linear power spectrum used for the Millennium simulation should correspond to that of *cmbeasy*. Referring to figure 9 of [36], the mapping:

$$\Delta_{cmbeasy}^2(k) \rightarrow \Delta_{Millennium}^2(k) : \quad \Delta_{Millennium}^2 = f_{cM}(\Delta_{cmbeasy}^2) = 1.183 \cdot \Delta_{cmbeasy}^2 \cdot k^{1-n_s} \quad (7.24)$$

of the linear power spectra would be appropriate for high k of about $k = 50 h Mpc^{-1}$ as it is shown in figure 7.2. There remains the need of an analytic continuation of the nonlinear power spectrum below scales which are not realized by the Millennium simulation. The high- k -approach of the nonlinear growth $\Delta_{NL}^2 = A_{x^{3/2}} (\Delta_L^2)^{3/2}$ will be used. A fit in the range $k \in [60 \dots 100] h Mpc^{-1}$ results in $A_{x^{3/2}} = 19.0973$ (also shown in figure 7.2).

Additionally a shift of the underlying scales was assumed, if the nonlinear regime is entered: $k_L = (1 + \Delta^2(k_{NL}))^{-\frac{1}{3}}$. But according to [42], I assume, that no scale shifting happens.

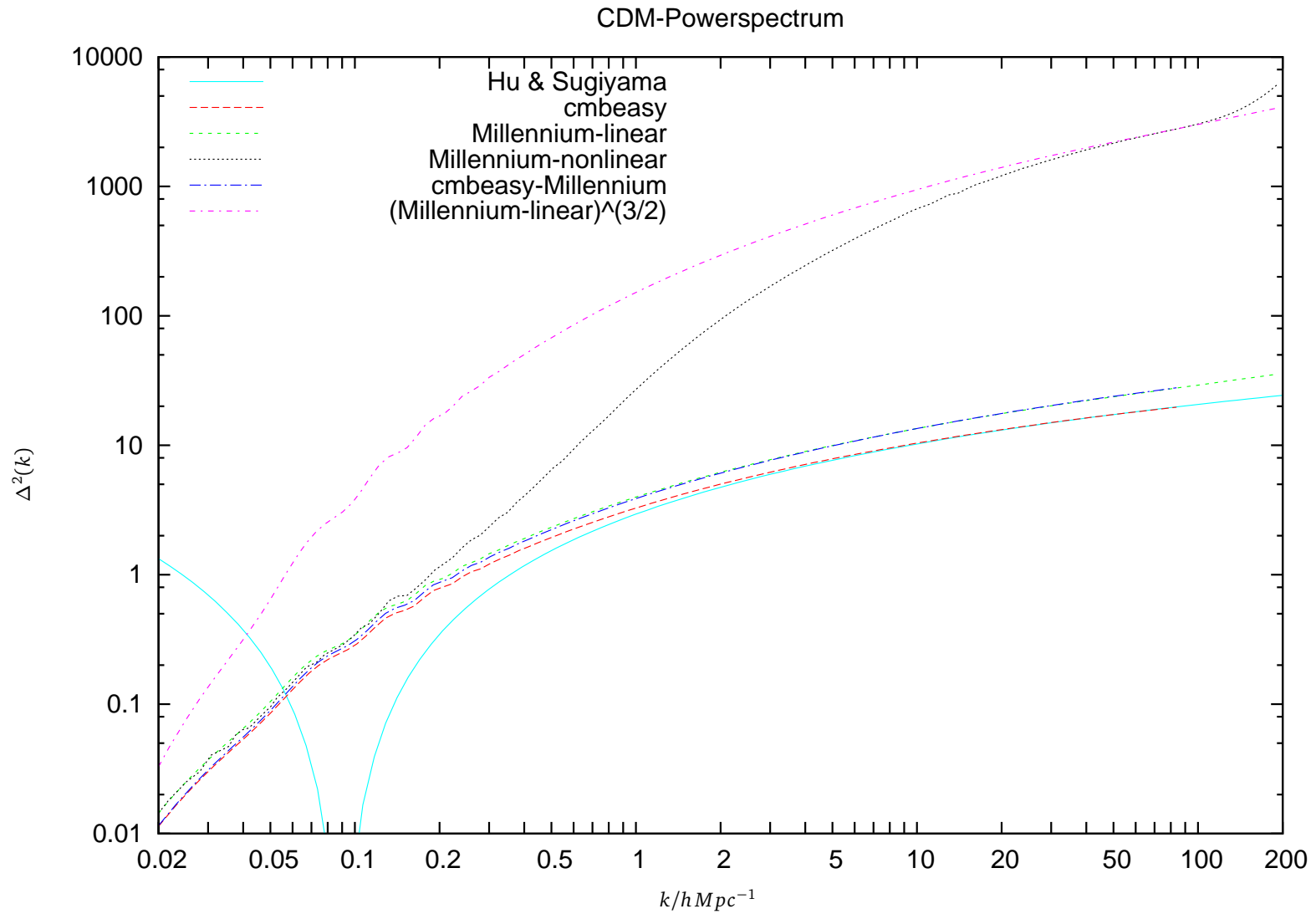


Figure 7.2: Preparational picture of the analytic continuation of the linear and nonlinear power spectra

'cmbeasy' is the CDM power spectra generated from cmbeasy with the fitted analytical continuation of 'Hu & Sugiyama'. To apply the nonlinear growth, the 'Millennium-linear' power spectrum is adjusted to the cmbeasy spectrum by the mapping $\Delta_M^2 = f_{cM}(\Delta_c^2)$ ('cmbeasy-Millennium'). The high- k -tail of the 'Millennium-nonlinear' power spectrum is fitted by the approximation $y' = y^{3/2}$ '(Millennium-linear)^{3/2}'. The small envelope at the end of the nonlinear power spectrum of the Millennium simulation maybe a numerical artefact. The rise of the 'Hu & Sugiyama' approach for small k originates from the general rise of $f(x) = \log^2(x)$ for small x .



8 The search for a cutoff

Now the question will be considered, if we may discover a cutoff in the power spectrum. From this one may conclude a scale, at which never fluctuations were produced during inflation.

8.1 The CMB

An obvious option is to consider the CMB power spectrum, shown in figure 8.1. The cutoff was introduced at the first peaks and was of the form $(1 + 10^{50 \cdot \log(k/k_0)})^{-1}$, representing nearly a sharp drop. Regarding the figure, it seems to be difficult to make out a cutoff in the CMB. The highest resolution coming from ACBAR is about $l = 3000$. According to equation 4.59 this corresponds to $15 Mpc$ or $k = 0.42 Mpc^{-1}$. The upcoming Planck satellite should be able to measure the power spectrum up to $l = 2160$ with a sensitivity of $\Delta T/T \approx 2.5 \cdot 10^{-6}$. Some disadvantages by searching for a cutoff in the CMB are:

1. The smaller the scales of the cutoff are (= high l) the more smooth is the deviation of the CMB, although a sharp cutoff was used.
2. The CMB is exponentially damped by the silk damping mechanism by linear increasing l . Therefore it would be more and more difficult to distinguish the CMB from other radio sources, like for example the milky way.
3. The CMBR is useful for explore huge scales. But the important small scales are rather difficult to resolve.

8.2 CDM power spectra

According to chapter 7, I propose an overall CDM spectrum of density fluctuations:

Linear regime: $k < 0.1 h Mpc^{-1}$

$$\Delta^2(k) := \Delta_{cmbeasy}^2(k) \quad (8.1)$$

Nonlinear regime: $k \in [0.1, 100.0] h Mpc^{-1}$

$$\Delta^2(k) := f_{cM}^{-1} \left[\Delta_{NL \text{ Millennium}}^2(k) \right] = 0.845 \cdot \Delta_{NL \text{ Millennium}}^2 \cdot k^{-0.04} \quad (8.2)$$

Asymptotic regime: $k > 100.0 h Mpc^{-1}$

$$\Delta^2(k) := f_{cM}^{-1} \left[A_{x^{3/2}} \left(f_{cM} \left(\Delta_L^2 \right) \right)^{3/2} \right] = 20.92 \Delta_L^3 k^{0.02}, \quad (8.3)$$

$$\Delta_L^2 = \frac{A k^{n_s+3} T^2(k)}{2\pi^2} = \frac{A k^{n_s+3} \left(0.89 \frac{\ln(15.9k)}{783k^2} \right)^2}{2\pi^2} = 0.498 \ln^2(15.9) \cdot k^{\frac{1-n_s}{2}}, \quad (8.4)$$

$$\Rightarrow \Delta^2(k) = 20.76 \left(0.498 \ln^2(15.9) \cdot k^{-(1-n_s)} \right)^{\frac{3}{2}} k^{\frac{1-n_s}{2}} = 7.296 \ln^3(15.9k) k^{-0.04} \quad (8.5)$$

This 'reference spectrum' should be valid up to very small scales. A deviation in form of a drop down would be a direct verification of a cutoff. A comparison of the reference spectrum with current observations has been done in figure 8.2. Whereas the data coming from SDSS lies well below the estimated power spectrum and may give an evidence for a cutoff, the Lyman alpha data is far above the spectrum. This is rather inappropriate, because Max Tegmark already produced a plot, shown in figure 8.3 at which all data fits the expectation very well. The Lyman alpha data reaches scales of about $k = 4 h Mpc^{-1}$, corresponding to $\lambda = 2,24 Mpc$ or $l = 20055$.

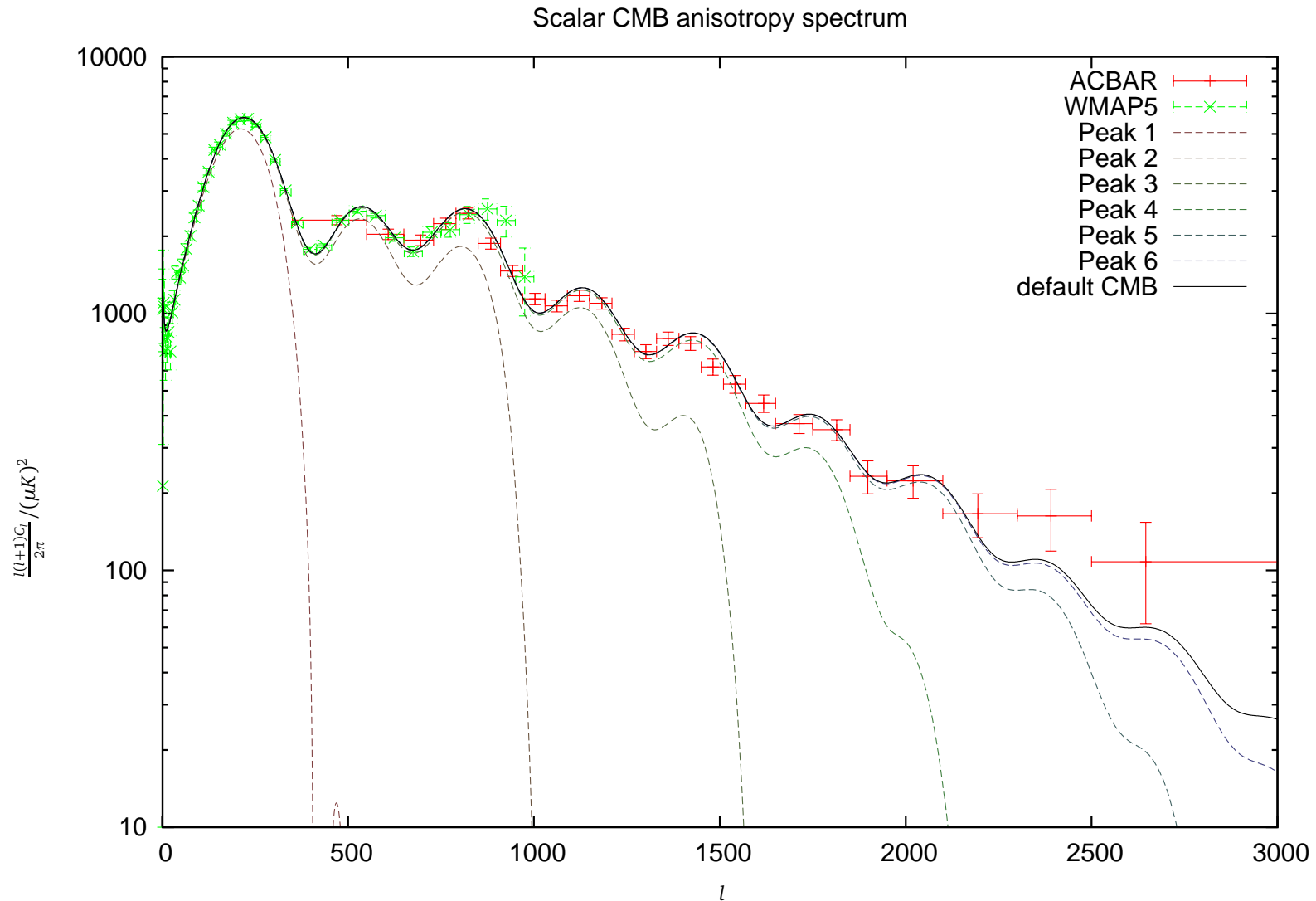


Figure 8.1: Cutoff in the CMB-anisotropy power spectrum?

In difference to the 'usual' CMB plots the y-axis is logarithmic and the x-axis non-logarithmic. This makes it easier to investigate the high l (small scales). The exponential Silk damping is also well resolved. The black solid line shows the default CMB power spectrum as it is calculated with `cmbeasy`. The dashed lines show cutoffs, introduced at the first to the sixth peak, which are appearing successively from the left to the right. The 'x' are the 5 year released binned data points measured by the WMAP satellite. The y-errors are taken from the Fischer matrix. The '+' are the binned data points released in 2008 by the ACBAR bolometer. There seems to be no evidence for a cutoff, which should occur at high l .

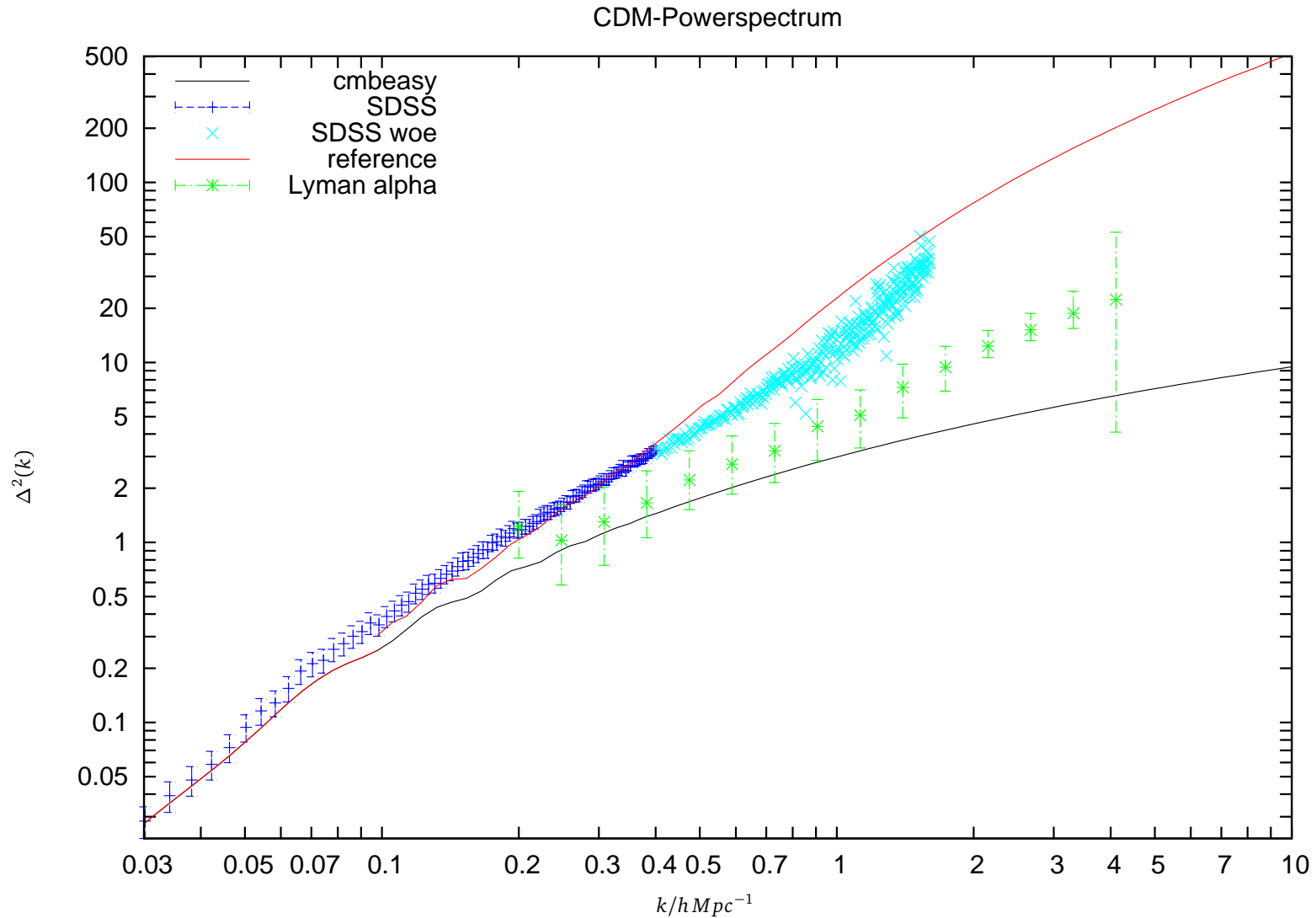


Figure 8.2: Comparison of the 'reference spectrum and measured data'

The red line, which changes in the black line shows the linear CDM power spectrum. The unsteady continuation of the nonlinear power spectrum (red line) emerges, because the adaption of the linear power spectra of cmbeasy and the one underlying to the Millennium simulation are tuned be in line at scales of $k = 60hMpc^{-1}$ and not at $k = 0.1hMpc^{-1}$. The blue and cyan dots are data from SDSS [40], where the error of the blue samples has been taken of figure 12 of [32]. The green samples are data of the intergalactic medium, obtained by investigating the Lyman alpha forest [41]. Note, that the nonlinear effects are already included in the $Ly\alpha$ data. Therefore it has to be compared with the linear power spectrum.

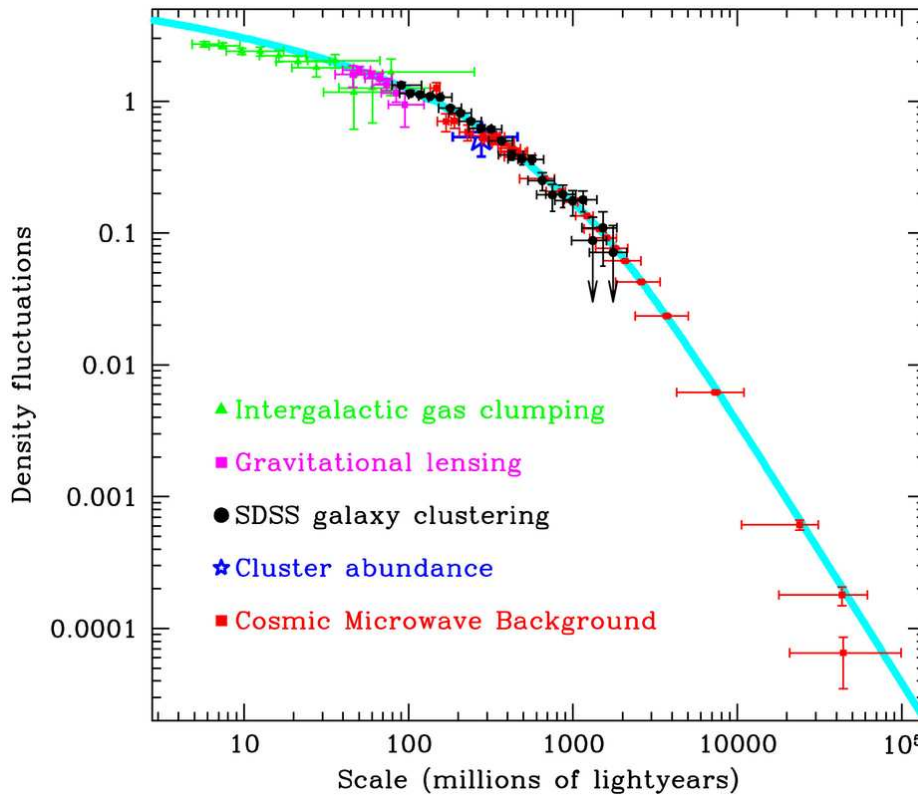


Figure 8.3: Density fluctuations of matter

This figure shows the density fluctuations $\langle \Delta^2 \rangle$, introduced in equation 7.2 by Max Tegmark [44]. Like in figure 8.2 it shows the data of intergalactic medium and the SDSS. Although the integral of the density fluctuations modifies the representation of the power spectrum, the data fits well on the theoretical predicted cyan line.

8.3 Luminosity function of galaxies

The luminosity function of galaxies (see figure 8.4) gives conclusions to the occurrence of matter structure formation on small scales. The expected luminosity function is related to the number of halo objects per logarithmic mass-scale. From figure 2 of [36] of the power spectrum ($n = 1$) based millennium simulation one concludes, that the so called halo multiplicity function $M^2 \rho^{-1} dn/dM = const$ is nearly constant over a wide range. The end of this constant behavior can be seen in figure 8.5, where the constancy of the halo multiplicity function is represented by the dashed-dotted line and the conversion $dn/d \log M = M^{-1} const$ has been applied. The mass-luminosity fraction is approximately constant: $(M/L)/(M_\odot/L_\odot) \approx 10$ as it can be concluded from [11] section 10.4.3. The corresponding luminosity function is plotted as dashed line in figure 8.4. Note, that according to the $M_{bol} - M_{bol\odot} = -2.5 \log(L/L_\odot)$ dependency of the absolute magnitude to the luminosity a change of $\Delta M = -7.5$ increases the luminosity by a factor 10^3 . Due to the cubic dependence of the mass to a given scale this corresponds to a change of the scale of a factor 10. A magnitude of $M = -22$ corresponds to a galaxy with about $m = 10^{12} M_\odot$ solar masses. Using the averaged mass density of the Friedmann universe today $\rho_b = 1.10 \cdot 10^{105} Mpc^{-4} = 4.26 \cdot 10^{-28} kg/m^{-3}$ (taken from the cmbeasy program) this mass scale has to be formed from a sphere with a radius of $r \approx 3.4 Mpc$.

In figure 8.4 one may find an evidence for a cutoff at scales of about $k = 90 h Mpc^{-1}$. However, to be sure, that this is a cutoff, than rather a natural effect, the formation of galaxies has to be more well understood.

8.4 Discussion

The above sections discussed that there seems to be no evident cutoff on wide ranges. It might be that there are fewer fluctuations on scales smaller than $\lambda = 100 kpc$. However, there seems to be an evidence that some kind of cutoff must exist: According to [43] the structure of the dark matter is conserved to very small scales. 50% of the dark matter is bound in haloes of 10^{-6} solar masses, corresponding to a scale of about $\lambda \approx 5 pc$. From figure 3 of [43] (see fig. 8.5) one can conclude that there should be about 10^{14} dark matter halo objects in the area of $1 h^{-3} Mpc^3$ having a mass of the earth. It is stated, that the earth should encounter such an object every 10000 years. But from astronomy there seems

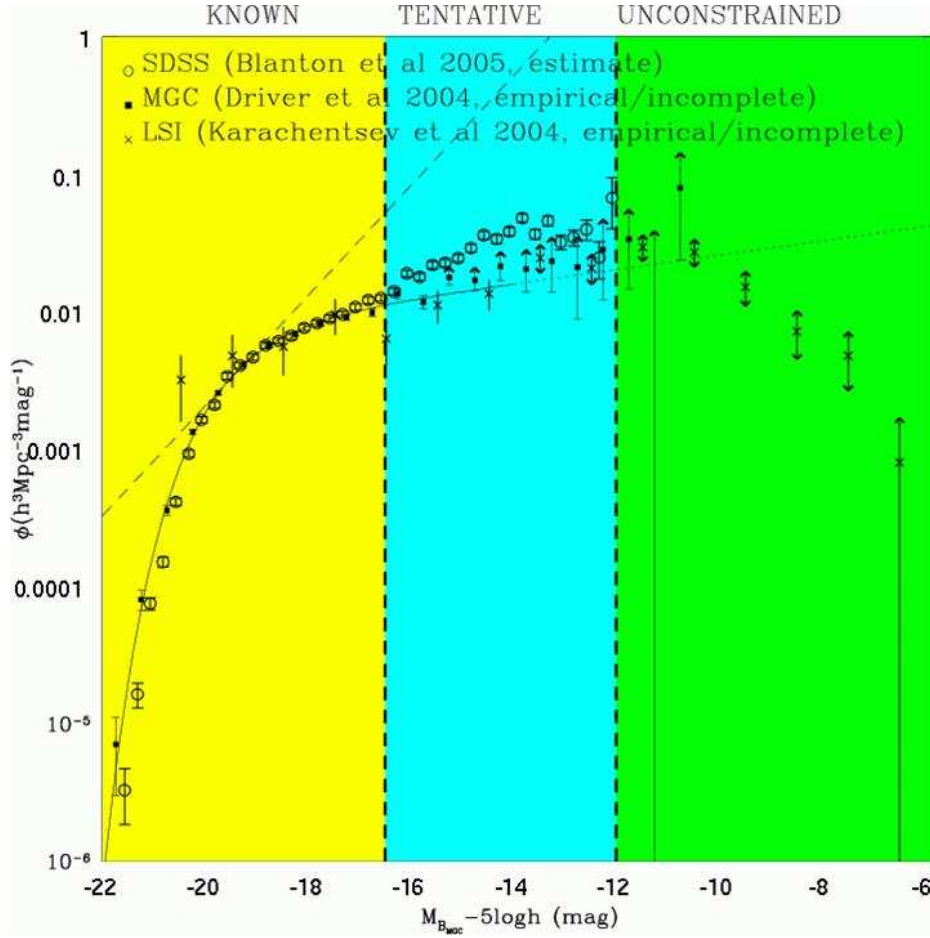


Figure 8.4: Luminosity function of galaxies Φ

Φ is defined as number of galaxies given in the specific volume $h^3 Mpc^{-3}$, whose luminosity ranges in a magnitude difference $\Delta M = 1$ and is therefore proportional to $dn/d \log M$. According to the text, magnitudes of $M = -22$ corresponds to objects with masses of $m = 10^{12} M_\odot$ with a scale of $r \approx 3.4 Mpc$ and $M = -7$ corresponds to $m = 10^6 M_\odot$ and $r \approx 34 kpc$. The plotted data is taken from [47], [48], [49]. A strong deviation of the expected dashed line occurs at about $M_B = -12$, corresponding to $\lambda = 100 kpc$, $k = 90 h Mpc^{-1}$ or $l = 4.51 \cdot 10^5$.

to be no evidence that there exist such a huge amount of 'small' only gravitationally acting objects. Thus one has to conclude that the primordial 'seed fluctuations', from which such dark matter haloes originate never existed.

What kind of conclusions can now be drawn from this observation for the Planck scale physics? The general idea of inflation physics is, that fluctuations are produced before and at horizon crossing. This means (see figure 8.6), that usually a small scale fluctuation is growing due to the strong Hubble expansion of $H = 6 \cdot 10^{-6} m_{pl}$ (see section 4.8.1) and is affected by fluctuations. At horizon crossing the fluctuations freeze out and remain untouched until the scale reaches the Hubble horizon again. Then the perturbations evolve according to cosmological perturbation theory, as it is implemented in cmbeasy. One might describe the generation of fluctuations of $\Delta_R(k)$ by using a rather phenomenological approach:

$$\Delta_R(l) = \int_{l_p}^{l_{hor} + \epsilon} F(a, l) d \ln l, \quad (8.6)$$

where the function $F(a, l) \geq 0$ is a fluctuation generation function, which is a function of the length scale l . To parameterize the 'time', at which the fluctuation generation happens, F is also a function of the comoving scale k . The interpretation of the integral is that a comoving scale k begins to grow from the Planck scale l_p to the horizon scale l_{hor} and a bit beyond. During this growth the comoving scale collects fluctuation contributions on every extension, then freezes at the horizon and remains unchanged until it enters the horizon again. The question comes up, what the properties of $F(a, l)$ are? The above consideration tells, that $F(a, l) = 0$, $\forall \lambda < 100 kpc$ should be the case. This might be interpreted as some kind of cutoff coming from the discretization of quantum gravity. This is remarkable, because one would expect, that the fluctuation generation process should stop in the first place on scales, that never leave the horizon, ie. the comoving

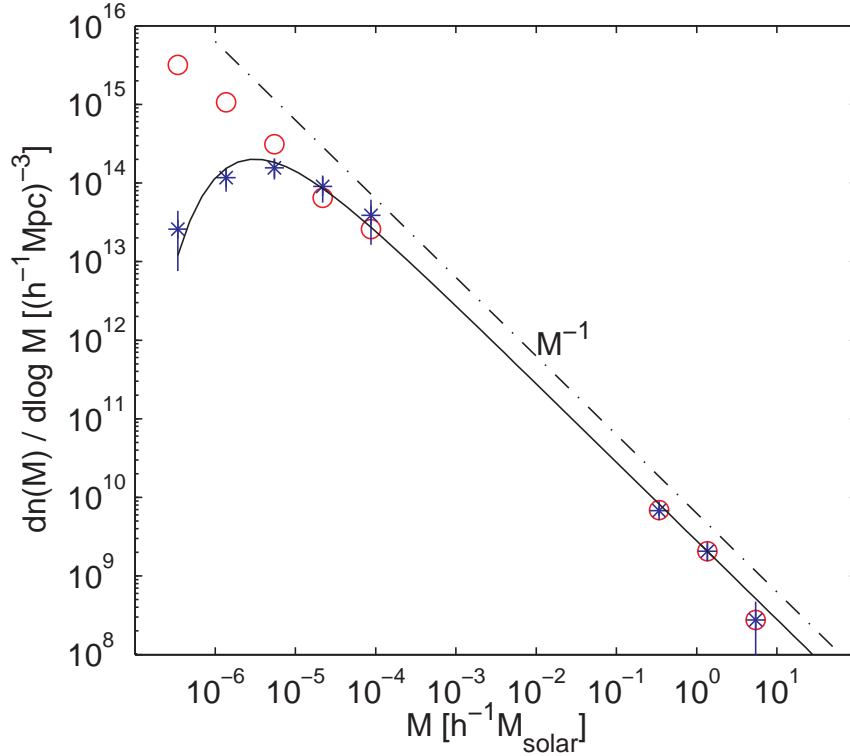


Figure 8.5: Occurrence of dark matter haloes at a given scale

This figure shows the number of dark matter haloes per logarithmic interval of a given mass-scale M . The dotted-dashed line shows the interpolation of the nonlinear power spectrum (see section 8.3). The solid line is a fit to the simulation data (stars), using a 100GeV neutralino dark matter particle. The circles show a simulation with axion dark matter. From this figure one concludes, that numerous dark-matter haloes of the mass of the earth $M \approx 10^{-6}M_{\odot}$ should exist, if the corresponding fluctuations during inflation happened.

scale $l = 1m$.

One can also see in figure 8.6 that the scales of physics that can be regarded by structure formation as it is treated in this work are very huge comoving scales today. Smaller comoving scales than about $5pc$ would be smeared out. Additionally one might ask the question, if the Fourier decomposed fluctuations can in fact evolve through the non-linear regime without affecting each other. Referring to the Millennium simulation one sees a very non-linear behavior of the structures, which are merging and twisting around. But Zhaoming Ma shows in his paper [42], that a cutoff is indeed conserved in particular in the non-linear regime. To go sure, that this behavior also occurs by having initially a cutoff power spectrum, a numerical N-body-simulation should be done. Only a direct proof would rule out (or confirm) any doubts that even in the non-linear regime every mode grows independently of each other.

8.4.1 Conventional generation of fluctuations

Anyhow, the treatment, given in equation 8.6 is only some kind of classical approach. In general one tries to quantize eq. 5.40, which can be obtained by the Lagrangian (refer to [3] and [28]):

$$\mathcal{L} = \frac{1}{2} \left((\dot{u})^2 - (\nabla u)^2 + \frac{\ddot{\theta}}{\theta} u^2 \right). \quad (8.7)$$

By introducing a canonical conjugate momentum and requiring the usual commutation relations, one ends up with the mode decomposition of the field operator:

$$\hat{u}(\eta, k) = (2\pi)^{-\frac{3}{2}} \int d^3k \left[u_k(\eta) \hat{a}_k e^{ik \cdot x} + u_k^*(\eta) \hat{a}_k^\dagger e^{-ik \cdot x} \right]. \quad (8.8)$$

Note, that the decomposition is along conformal time and not the physical time. According to the expansion of space, the physical vacuum has to be defined on every time individually. Therefore the mode amplitudes $u_k(\eta_0)$ are related by a

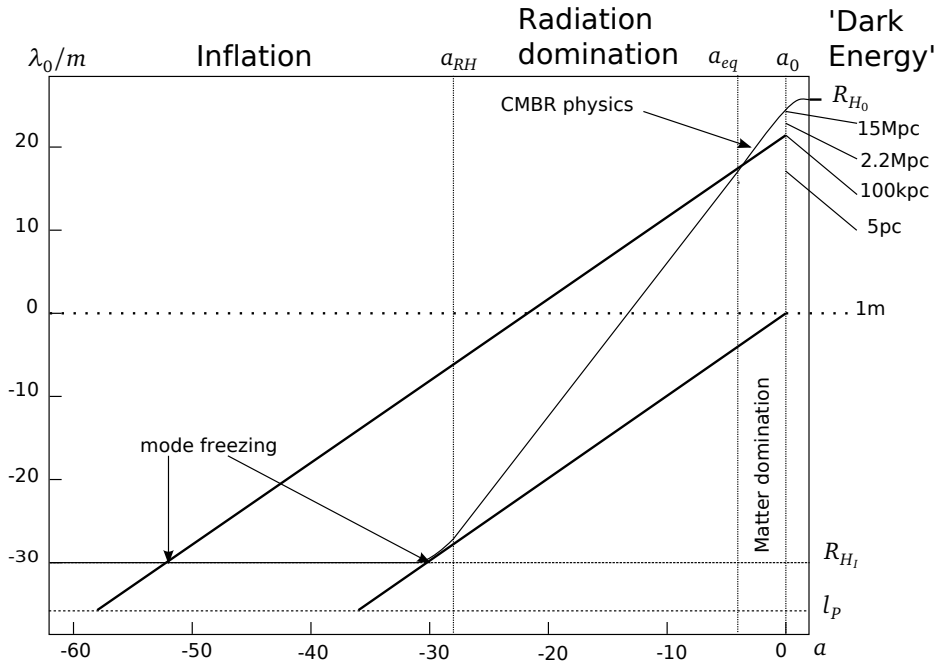


Figure 8.6: Evolution of comoving scales and horizon scales

The length scales λ are plotted over the scale factor a . The thick, solid, diagonal lines are comoving scales. The solid line shows the horizon scale, which is approximately constant during inflation, growing during matter and radiation domination due to deceleration of the universe expansion and gets constant again today, due to dark energy domination. The dotted line shows the Planck length.

Bogoliubov transformation to amplitudes of earlier and later times. The power spectrum then depends on the two point correlation function of \hat{u} , whose mode amplitudes are related to the inflation dynamics.

However, a precise prediction of the power spectrum generated during inflation could only be made by using an underlying theory of quantum gravity.

8.4.2 Conclusions

From figure 8.6 one sees that the about first 10 orders of magnitude of the 26 orders lasting inflationary expansion can be constrained by observing the structure formation today. The cutoff, found at a scale of about $100kpc$ would imply, that fluctuations were generated during the first 7 orders of magnitude during inflation. The next 3 orders haven't obviously produced any fluctuations. The rest of the inflationary expansion cannot be constrained by observing the structure of the universe.

These conclusions can only be drawn, if two assumptions hold:

1. Small scale structures remain existent, even if they pass the non-linear regime of structure formation.
2. Small scale dark matter objects would affect the physics, we are observing. This means for example, that deviations of the relativistic Keplerian motion of astronomic bodies should occur.

Referring to the motivating text for this work in the introduction, I see no direct possibility to give constraints to the scale of a quantum gravity cutoff from astronomical structure. In this context a quantum gravity cutoff means the characteristic energy scale, at which the space-time may become discrete. The answer of scales at which inflation has generated fluctuations can instead be given.



9 Acknowledgements

First I'd like to thank Professor Max Camenzind for his supervision. He was always available for questions and discussed everything very friendly. Also grateful acknowledges to Professor Jürgen Berges, who gave some helpful suggestions to me, concerning my work.

I'd also like to mention the staff of the theory group of the Landessternwarte Heidelberg. I had a lot of useful and nice discussions with all members.



Descriptions

Acbar: Arcminute Cosmology Bolometer Array Receiver
Radio interferometry experiment of the CMBR

BAO: Baryonic Acoustic Oscillations
In the early universe the density fluctuations of dark matter generate a gravitational potential, in which the baryonic matter performs acoustic oscillations. These oscillations depend on the density parameters of the universe.

CBI: Cosmic Background Imager
Radio interferometry experiment of the CMB

CMB: Cosmic Microwave Background

CMBR: Cosmic Microwave Background Radiation

ISW: Integrated Sachs Wolfe effect
A temperature shift in the CMB caused by a time variation of the potentials Ψ , Φ .

LRG Luminous Red Galaxies
Special distant objects observed by SDSS.

OSW: Ordinary Sachs Wolfe effect
A temperature shift in the CMB caused by climbing out of the gravitational potential Ψ , Φ .

SN 1a: Type 1a Supernovae
A white dwarf, which exceeds its mass-limit and starts a nuclear carbon fusion. The luminosity of these stars is well known and can be used for obtaining the luminosity distance.

SDSS: Sloan Digital Sky Survey
SDSS is a redshift survey which aims to observe 100 million objects on the sky.

SUSY: SUperSYmmetry
A symmetry used in particle physics, to unify the three fundamental interactions electro-magnetisms and the weak and strong force by introducing super partners to every particle.

WMAP: Wilkinson Microwave Anisotropy Probe
A satellite, which measured the CMBR-Anisotropies. In particular the first peak in the CMB- C_l -Power spectrum is measured by WMAP.

Erklärung zur Bachelor Thesis gemäß §23 Abs. 7 APB:

Hiermit versichere ich, die vorliegende Master Thesis ohne Hilfe Dritter nur mit den angegebenen Quellen und Hilfsmitteln angefertigt zu haben. Alle Stellen, die aus den Quellen entnommen wurden, sind als solche kenntlich gemacht worden. Diese Arbeit hat in gleicher Form noch keiner Prüfungsbehörde vorgelegen.

Bibliography

- [1] Clifford M. Will, “The Confrontation between General Relativity and Experiment”, *Living Rev. Relativity*, 9, (2006), 3. , <http://www.livingreviews.org/lrr-2006-3>
- [2] Norbert Straumann, “General Relativity”, “With Applications to Astrophysics”, *Springer Verlag Berlin Heidelberg*, (2004)
- [3] Norbert Straumann, “From Primordial Quantum Fluctuations to the Anisotropies of the Cosmic Microwave Background Radiation”, (2006), [arXiv:hep-ph/0505249]
- [4] Ruth Durrer, “Cosmological Perturbation Theory”, (2004), <http://mpej.unige.ch/~durrer/courses/syros.pdf>
- [5] Mikio Nakahara, “Geometry, Topology and Physics”, *Taylor and Francis Group, Great Britain*, (2003)
- [6] Christian Bär, “Elementare Differential Geometrie”, *de Gruyter, New York*, (2001)
- [7] Max Camenzind,
<http://www.lsw.uni-heidelberg.de/projects/theory/resource.htm>
- [8] Max Camenzind, “General Relativity”, Chapter 4, (2004), http://www.lsw.uni-heidelberg.de/users/mcamenzi/GR_04.pdf
- [9] Max Camenzind, “From Big Bang to Black Holes”, Chapter 3, (2003), http://www.lsw.uni-heidelberg.de/users/mcamenzi/BigBang_03.pdf
- [10] Max Camenzind, “From Big Bang to Black Holes”, Chapter 4 (2003), http://www.lsw.uni-heidelberg.de/users/mcamenzi/BigBang_04.pdf
- [11] Max Camenzind, “Astronomie and Astrophysik II”, Chapter 10 (2006), http://www.lsw.uni-heidelberg.de/users/mcamenzi/APII_Lect10.ps.gz
- [12] Matthias Bartelmann, “General Relativity”, <http://www.ita.uni-heidelberg.de/~msb/Lectures/relativity/relativity.pdf>
- [13] Sean M. Carroll, “Lecture Notes on General Relativity”,(1997) , [arXiv:gr-qc/9712019]
- [14] Petr K. Raschewski, “Riemannsche Geometrie und Tensoranalysis”, 2nd edition, *Harri Deutsch, Frankfurt am Main, Thun*, (1995)
- [15] Bengt Friman, “Introduction to the General Theory of Relativity”, (2006), <http://theory.gsi.de/~friman/gtr-script/script.html>
- [16] Andrew Liddle, “An Introduction to Modern Cosmology”, *Wiley* , 2 edition, (2003)
- [17] Ericourgoulhon, “3 + 1 Formalism and Bases of Numerical Relativity”, (2007), [arXiv:gr-qc/0703035]
- [18] Ken-ji Hamada, “Resummation and Higher Order Renormalization in 4D Quantum Gravity”, (2002), [arXiv:hep-th/0203250]
- [19] Ken-ji Hamada1 , Shinichi Horata and Tetsuyuki Yukawa, “Space-time Evolution and CMB Anisotropies from Quantum Gravity”, (2006), [arXiv:astro-ph/0607586]
- [20] Ken-ji Hamada1 , Shinichi Horata , Naoshi Sugiyama, Tetsuyuki Yukawa4, “Analyzing WMAP Observation by Quantum Gravity”, (2007), [arXiv:astro-ph/0705.3490]
- [21] E. Komatsu, J. Dunkley, M. R.olta et al. , “Five-year Wilkinson Microwave Anisotropy Probe (WMAP) observations: Cosmological interpretation”, (2008), [arXiv:astro-ph/0803.0547]
- [22] Adam G. Riess , Louis-Gregory Strolger , John Tonry et al. , “Type Ia Supernova Discoveries at $z > 1$ From the Hubble Space Telescope: Evidence for Past Deceleration and Constraints on Dark Energy Evolution”, (2004), [arXiv:astro-ph/0402512]

-
- [23] The Planck collaboration, “The Scientific Programme of Planck”, (2006), [arXiv:astro-ph/0604069]
- [24] Ue-Li Pen, “Brief Note: Analytical Fit to the Luminosity Distance for Flat Cosmologies with a Cosmological Constant”, (1999), [arXiv:astro-ph/9904172]
- [25] Lecture by Michael Doran, “A Primer on Cosmology and the Cosmic Microwave Background”, www.cmbeasy.org
- [26] Michael Doran, Christian M. Müller, Gregor Schäfer et al., “Gauge Invariant Initial Conditions and Early Time Perturbations in Quintessence Universes”, (2003), [arXiv:astro-ph/0304212]
- [27] Hideo Kodama and Misao Sasaki, “Cosmological Perturbation Theory”, *Progress of Theoretical Physics Supplement*, 78, (1984)
- [28] Viatcheslav Mukhanov, “Physical Foundations of Cosmology”, *Cambridge University Press*, (2005)
- [29] Chung-Pei Ma, Edmund Bertschinger, “Cosmological Perturbation Theory in the Synchronous and Conformal Newtonian Gauges”, (1995), [arXiv:astro-ph/9506072]
- [30] Andrew Liddle and David Lyth, “The Cold Dark Matter Density Perturbation”, (1993), [arXiv:astro-ph/9303019v1]
- [31] Kandaswamy Subramanian, “The Physics of CMBR Anisotropies”, (2004), [arXiv:astro-ph/0411049]
- [32] Will J. Percival, Robert C. Nichol, Daniel J. Eisenstein et al., “The Shape Of The SDSS DR5 Galaxy Power Spectrum”, (2006), [arXiv:astro-ph/0608636]
- [33] Wayne Hu and Naoshi Sugiyama, “Anisotropies in the Cosmic Microwave Background: An Analytic Approach”, (1995), *The Astrophysical Journal*, 444: 489-506
- [34] Wayne Hu and Naoshi Sugiyama, “Toward understanding CMB anisotropies and their implications”, (1995), *Phys. Rev.*, Vol. 51: Nr.6
- [35] Wayne Hu and Naoshi Sugiyama, “Small Scale Cosmological Perturbations: An Analytic Approach”, (1996), [arXiv:astro-ph/9510117]
- [36] V. Springel, S. D. M. White, A. Jenkins, “Simulating the joint evolution of quasars, galaxies and their large-scale distribution”, (2005), [arXiv:astro-ph/0504097]
- [37] A. J. S. Hamilton, P. Kumar, Edward Lu and Alex Matthews, “Reconstructing the Primordial Spectrum of Fluctuations of the Universe from the Observed Nonlinear Clustering of Galaxies”, (1991), *The Astrophysical Journal*, 374: L1-L4
- [38] J.A. Peacock and S.J. Dodds, “Nonlinear evolution of cosmological power spectra”, (1996), [arXiv:astro-ph/960303]
- [39] R.E. Smith, J.A. Peacock, A. Jenkins et al. “Stable clustering, the halo model and nonlinear cosmological power spectra”, (2002), [arXiv:astro-ph/0207664]
- [40] Will Percival, <http://www.dsg.port.ac.uk/~percivalw/>
- [41] S. Zaroubi, M. Viel, A. Nusser et al., “The matter power spectrum at small scales: an estimate from the Ly α forest optical depth”, (2005), [arXiv:astro-ph/0509563]
- [42] Zhaoming Ma, “The nonlinear matter power spectrum”, (2006), [arXiv:astro-ph/0610213]
- [43] J. Diemand, Ben Moore and J. Stadel, “Earth-mass dark-matter haloes as the first structures in the early Universe”, (2005), [arXiv:astro-ph/0501589]
- [44] Max Tegmark, <http://space.mit.edu/home/tegmark/sdss.html>
- [45] Shinji Tsujikawa, “Introductory Review of Cosmic Inflation”, (2003), [arxiv:hep-th/0304257]
- [46] Andrew R. Liddle and David H. Lyth, “Cosmological Inflation and Large-Scale Structure”, (2000), Cambridge University Press
- [47] I. K. Baldry, K. Glazebrook, T. Budavari et al., “The SDSS u-band Galaxy Survey: Luminosity functions and evolution”, (2005), [arxiv:astro-ph/0501110]

-
-
- [48] Simon P Driver, Paul D. Allen, Jochen Liske et al., “The Millennium Galaxy Catalogue: The luminosity functions of bulges and discs and their implied stellar mass densities”, (2007), [arxiv:astro-ph/0701728]
- [49] I.D. Karachentsev, V. E. Karachentseva, W. K. Huchtmeier et al., “A Catalog of Neighboring Galaxies”, (2004), The Astronomical Journal, 127, 2031-2068